ISSN 1331-7210

1993. 2018.

Engineering Power

BULLETIN OF THE CROATIAN ACADEMY OF ENGINEERING Vol. 12(3) 2017

Euro-CASE

CAETS

EDITOR-IN-CHIEF'S WORD

Dear Readers,

We are very pleased to present you the new issue of our Academy's Bulletin in English ***„Engineering Power"*** Vol. 12(3) 2017, which has been guest-edited by Zdravko Virag, Member of the Academy in the Department of Mechanical Engineering and Naval Architecture.

One of the principal goals of our Academy, apart from the promotion and popularization of technological and biotechnological sciences, is to promote interdisciplinary approaches to solving engineering problems, which result in cutting-edge technologies that will shape future scientific improvements. "Engineering Power" is one of our selected media through which we hope to draw your attention to the efforts and achievements of our Academy and its members.

Editor-in-Chief
Vladimir Andročec, President of the Croatian Academy of Engineering

EDITOR'S WORD

Croatian Academy of Engineering, as the only scientific institution in the Republic of Croatia that brings together scientists and researchers of all profiles in technological and biotechnological sciences, especially encourages interdisciplinary co-operation in particular fields as one of the principal leverages of scientific and technological development. We are also witnessing the emphasizing of interdisciplinary priorities of research topics in the field of application of research projects to domestic and international scientific grant application procedures and programs, such as Croatian Science Foundation and Horizon 2020.

Although this trend is visible in a number of research fields, both in fundamental and applied ones, the interconnection of technological and biomedical disciplines is a distinct *success story* of contemporary science.

The advancement in their complementation and rapid development based on mutual stimulation and even permeation, such as in some cases where the technical and technological part of research is inseparable from its biomedical constituent and vice versa, has contributed to the development of treatment and diagnostics techniques that have significantly improved the contemporary quality of life and were almost inconceivable just a few years ago.

In that regard, the Croatian Academy of Engineering is especially pleased to present in two subsequent issues of its Bulletin „Engineering Power" a part of research activities that are being conducted at the University of Zagreb, and that synergically combine technological and biotechnological sciences. The invited editors are leaders of the research teams at the University of Zagreb Faculty of Mechanical Engineering and Naval Architecture. In research activities the teams are associated with colleagues from the University of Zagreb, Faculty of Medicine as well as with distinguished international institutions.

It is my great pleasure to announce Prof. Zdravko Virag, PhD, the invited editor of the expert part of this issue, the first in the sequence. Prof. Zdravko Virag, PhD, Member of the Academy, is the Head of the Department of Fluid Mechanics at the Faculty of Mechanical Engineering and Naval Architecture, and the leader of the research group in the field of hemodynamic modeling of the cardiovascular system.

Editor
Zdravko Terze, Vice-President of the Croatian Academy of Engineering

FOREWORD

Biomedical engineering is one of the fastest developing fields, which touches many specialties and provides a basis for the faster development of medical science. Close and fruitful cooperation of medical doctors and engineers results in team synergy, thus enabling faster progress than in the case when everyone works separately in their own "silos". At the University of Zagreb, Faculty of Mechanical Engineering and Naval Architecture we recognized the necessity of such cooperation more than ten years ago. Today, our several engineer teams are teamed up with medical doctors in projects related to medicine. As pathological conditions in the cardiovascular system (such as atherosclerosis, formation of aneurysms, valvular heart diseases, etc.) are strongly interlinked with the hemodynamics of the cardiovascular system and tissue remodeling, they attract interest of our departments. The Department of Fluid Mechanics is now in charge of hemodynamics and the Department of Mechanics is in charge of tissue remodeling and formation of aneurysms.

The papers below provide the Department of Fluid Mechanics team with a short overview over research activities and results in the field of hemodynamic modeling of the cardiovascular system. We have developed models and numerical methods with different levels of complexity: from a lumped parameter model to one-dimensional and quasi two-dimensional to three-dimensional model. The simplest lumped parameter model is important for clinicians, since it describes the principal part of the cardiovascular system with a relatively small number of parameters, each having a clear physiological meaning crucial to understand the system function. Such a model is being applied in an ongoing project considering a non-invasive method for the model parameter identification of pulmonary circulation in subjects with pulmonary hypertension. The problem with one-dimensional and three-dimensional models is that they require more input data (e.g. space variation of blood vessel diameter and wall properties) that cannot be easily measured, but still such models are very important for understanding wave phenomena in the arterial tree and for estimating the local flow parameters, important for the prediction of some diseases (such as aneurysm growth). The developed models and methods are a good basis for prospective cooperation with other medical and engineering teams. Recently, we have established the Laboratory for Artificial Cardiovascular Circulation in cooperation with the University of Zagreb, School of Medicine with the purpose of collaborative research on artificial heart development and education of prospective medical engineering students.

Guest-Editor
Zdravko Virag, University of Zagreb, Faculty of Mechanical Engineering and Naval Architecture

Zdravko Virag[1], Fabijan Lulić[2]

A Lumped Parameter Model of the Cardiovascular Circulation

[1] University of Zagreb, Faculty of Mechanical Engineering and Naval Architecture,
[2] University of Zagreb, Pulmonary Disease Clinic

CONTENTS

Introduction

Cardiovascular diseases cause the majority of deaths in the developed countries. They are strongly interlinked with hemodynamics of the cardiovascular system (CS); thus it is important to study blood flow under normal and pathological conditions. Hemodynamic models of CS can be classified as lumped parameter, one-dimensional, two-dimensional and three-dimensional models. The simplest lumped parameter models are attractive for teaching purposes as well as for clinicians, since they describe the whole CS with a small number of parameters (in terms of compliance, resistance and inertance) having a clear physiological meaning. The results of such a model include pressure and volume time variations of observed compartments and also flow rates between compartments (arterial and vein trees are considered as compartments, too). Upgraded with a short-term regulatory system model (arterial baroreflex system, cardiopulmonary baroreflex system and neural control of the heart rate) and resting physiologic perturbations model, the resulting lumped parameter model is capable of generating pretty realistic results, and can be used for the research on the CS [1,2]. In the CVsim model [2] six compartments are used for the teaching version and 21 compartments in the research version, while the CircAdapt model [3] consists of eight compartments. The valves are considered to be ideal check valves in most models, and valve dynamics is modeled in [4]. A lumped model of the heart was developed in combination with one-dimensional model of blood vessel tree [5], and further there is a model with oxygen transport [6].

The goal of this work is to develop a simple hydrodynamic lumped parameter model of the cardiovascular system which can realistically describe time varying pressure in system compartments and flows through the valves in the given physiological state of the system. The model includes four heart compartments (left and right atria and ventricles) and systemic and pulmonary circulation (modeled by arterial and venous compartments). Heart contractility is modeled by time varying elastance [7] (frequently defined as the universal one for all subjects) in most existing models, while in this work the formulation with activation function is used for this purpose. Activation function is defined by parameters that can be obtained by Doppler Echocardiography specifically for each subject.

Mathematical model

A simplified CS (Fig. 1) is reduced to a system of eight chambers, as follows: pulmonary veins (PV), left atrium (LA), left ventricle (LV), systemic arteries (SA), systemic veins (SV), right atrium (RA), right ventricle (RV) and pulmonary artery (PA). Each chamber is characterized by volume (V) and pressure (p), while the blood flowrate (Q) is defined by eight connections between the chambers. These eight connections are: entrance from pulmonary veins into the left atrium (la), mitral valve (mv), aortic valve (av), systemic capillaries (sc), entrance to the right atrium (ra), tricuspid valve (tv), pulmonary valve (pv) and pulmonary capillaries (pc). For the sake of simplicity, it is assumed that pressure disturbances spread at infinite speed, resulting in uniform pre-

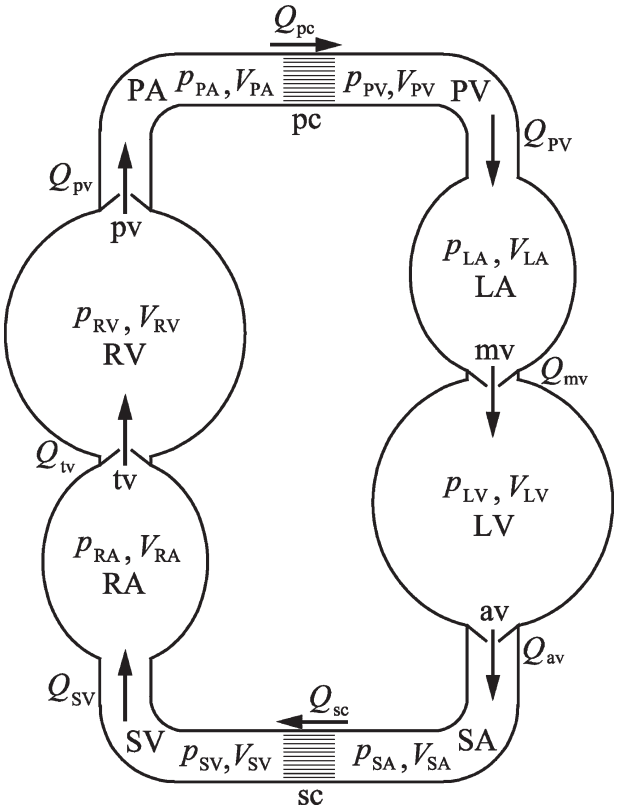

Fig. 1. Scheme of the cardiovascular system consisting of eight chambers and eight interconnections. Abbreviations: PV/SV = pulmonary/systemic veins, LA/RA = left/right atrium, LV/RV = left/right ventricle, SA/PA = systemic/pulmonary arteries, sc/pc = systemic/pulmonary capillaries, mv = mitral valve, av = aortic valve, tv = tricuspid valve, pv = pulmonary valve

ssure in each chamber is uniform. Arteries and veins are considered to be passive chambers (not adding energy to the blood flow), and the left and right heart chambers (atria and ventricles) are active chambers that add energy to the blood flow by their contraction. Blood is considered to be an incompressible fluid of constant density $\rho = 1050\ \mathrm{kg/m^3}$.

The continuity equation defines the rate of chamber volume change:

$$\frac{\mathrm{d}V}{\mathrm{d}t} = Q_{\mathrm{in}} - Q_{\mathrm{out}}\,, \tag{1}$$

where Q_{in} and Q_{out} are the inlet and outlet flow rate, respectively. For example, for pulmonary veins (PV) in Fig. 1 the continuity equation reads: $\mathrm{d}V_{\mathrm{PV}}/\mathrm{d}t = Q_{\mathrm{pc}} - Q_{\mathrm{PV}}$, for the left atrium (LA) it is: $\mathrm{d}V_{\mathrm{LA}}/\mathrm{d}t = Q_{\mathrm{la}} - Q_{\mathrm{mv}}$, and so on. Flow rate between two chambers is defined by the modified Bernoulli equation, which in the case of laminar fluid flow through the pipe of length L and diameter D, takes the form:

$$M\frac{\mathrm{d}Q}{\mathrm{d}t} = p_{\mathrm{in}} - p_{\mathrm{out}} - RQ - rQ^2\,, \tag{2}$$

where M is inertance coefficient, $M = \rho L/A$ ($A = D^2\pi/4$), $R = 32\mu L/\left(D^4\pi\right)$, μ is blood viscosity, $r = 8\rho K/\left(D^4\pi^2\right)$, and K is minor loss coefficient. It is convenient to neglect minor losses ($r = 0$) for the flows through systemic and pulmonary capillaries where friction losses are large, while friction loses are negligible ($R = 0$) with respect to minor losses in flows through valves. All valves are considered to be an ideal check-valve: the valve opens instantaneously for positive flow direction, and it closes instantaneously when flow direction tends to be negative.

Pressure-volume relationships

Veins and arteries models

Veins are modeled as vessels with elastic wall. If we define pressure as a pressure difference of inner vessel and interstitial pressure, then the pressure-volume relationship for veins reads:

$$p = E_0\left(V - V_0\right), \tag{3}$$

where E_0 is venous wall elastance and V_0 is blood volume in veins at zero pressure.

Arteries are modeled as vessels with a visco-elastic wall, and the pressure volume relationship, according to the Voigt model is:

$$p = E_0\left(V - V_0\right) + \eta\frac{\mathrm{d}V}{\mathrm{d}t}\,, \tag{4}$$

where η is arterial wall resistance.

Models of atria and ventricles

The walls of atria and ventricles contain muscles which contract after activation, and in that way they provide the driving force for blood flow. We distinguish two states of the wall: passive and active. The passive (or diastolic) state is modeled by a nonlinear passive pressure – volume relationship ($p_{\mathrm{d}} - V$):

$$p_{\mathrm{d}} = E_0 V_k\left(e^{\frac{V-V_0}{V_k}} - 1\right)\,, \tag{5}$$

where E_0 and V_0 are wall elastance and volume at zero pressure, respectively, and V_k is volume constant. In this model wall elastance (E_{d}) is volume (or pressure) dependent and thus it holds:

$$E_{\mathrm{d}} = \frac{\mathrm{d}p_{\mathrm{d}}}{\mathrm{d}V} = E_0 e^{\frac{V-V_0}{V_k}}\,. \tag{6}$$

The activation of muscles in the ventricular or atrial wall results in an additionally developed pressure, which should be added to passive pressure, resulting in total pressure:

$$p = p_{\mathrm{d}} + \alpha\left(p_{\mathrm{s}} - p_{\mathrm{d}}\right), \tag{7}$$

where α is time dependent activation function in the range from zero to one ($\alpha = 0$ denotes passive state and $\alpha = 1$ the end of systole). p_{s} is usually considered to be linear ESPVR (End Systolic Pressure-Volume Relationship), and here we added a quadratic term; thus, the expression for p_{s} is:

$$p_{\mathrm{s}} = E_0\left(V - V_0\right) + E_V V^2\,, \tag{8}$$

where E_V is constant coefficient.

During systole, when heart muscles contract, activation function rises from zero (at the beginning of systole) to one (at the end of systole), and after that it goes back to zero (relaxation). Here, we defined $t = 0$ at the beginning of systole, and we modeled activation function with a piecewise function:

$$\begin{aligned}
&\alpha^{\mathrm{I}} = A_1 t^2 \exp\left[A_2\left(t - t_{\mathrm{eivc}}\right)\right] && \text{for } 0 < t \le t_{\mathrm{eivc}}\\
&\dot{\alpha}^{\mathrm{II}} = A_3 + \left(1 - \frac{t - t_{\mathrm{eivc}}}{t_{\mathrm{es}} - t_{\mathrm{eivc}}}\right)\left(\dot{\alpha}_{\mathrm{eivc}} - A_3\right)\exp\left(A_4\left(t - t_{\mathrm{eivc}}\right)\right) - \\
&\quad - A_3\frac{t - t_{\mathrm{eivc}}}{t_{\mathrm{es}} - t_{\mathrm{eivc}}}\exp\left(A_4\left(t - t_{\mathrm{eivc}}\right)\right) && \text{for } t_{\mathrm{eivc}} < t \le t_{\mathrm{es}}\\
&\dot{\alpha}^{\mathrm{III}} = \frac{\alpha_{\mathrm{ee}}\left(t - t_{\mathrm{es}}\right)}{t_{\mathrm{ee}} - t_{\mathrm{es}}}\exp\left(A_5\left(t - t_{\mathrm{ee}}\right)\right) && \text{for } t_{\mathrm{es}} < t \le t_{\mathrm{ee}}\\
&\alpha^{\mathrm{IV}} = \alpha_{\mathrm{ee}}\exp\left(\frac{t_{\mathrm{ee}} - t}{\tau}\right) && \text{for } t > t_{\mathrm{ee}}
\end{aligned} \tag{9}$$

At time $t = 0$ (the beginning of the isovolumic contraction) $\alpha = 0$ and its time derivative $\dot{\alpha} = \mathrm{d}\alpha/\mathrm{d}t = 0$. Isovolumic contraction lasts up to time t_{eivc} (eivc = end of isovolumic contraction), when the aortic valve opens and activation function, and its time derivative take values $\alpha = \alpha_{\mathrm{eivc}}$ and $\dot{\alpha} = \dot{\alpha}_{\mathrm{eivc}}$, respectively. At the time of end-systole (t_{es}), interpolation function reaches its maximum value $\alpha = 1$, $\dot{\alpha} = 0$. After that, activation function decreases and at the time of end-ejection (t_{ee}) it gets a value of $\alpha = \alpha_{\mathrm{ee}}$. At t_{ee} time the aortic valve closes, and after that the isovolumic relaxation of the left ventricle starts. It is broadly accepted that during isovolumic relaxation the pressure falls according to the exponential law [8]: $p = p_{\mathrm{ee}}\exp(-t/\tau)$, where τ denotes isovolumic relaxation time constant, so it is reasonable to accept that activation function also follows the exponential law.

In Eq. (9) five unknown constants (A_1 to A_5) and two additional constants (A_6 and A_7) appear after integration expressions for $\dot{\alpha}^{II}$ and $\dot{\alpha}^{III}$. These seven constants are defined by seven conditions of continuity of α, $\dot{\alpha}$ and $\ddot{\alpha}$ as follows:

$$\begin{aligned}
&\alpha^{I}(t_{eivc}) = \alpha_{eivc} \\
&\alpha^{II}(t_{eivc}) = \alpha_{eivc} \\
&\dot{\alpha}^{I}(t_{eivc}) = \dot{\alpha}^{II}(t_{eivc}) \\
&\alpha^{II}(t_{es}) = 1 \\
&\alpha^{III}(t_{es}) = 1 \\
&\dot{\alpha}^{III}(t_{ee}) = -\alpha_{ee}/\tau \\
&\ddot{\alpha}^{II}(t_{es}) = \ddot{\alpha}^{III}(t_{es})
\end{aligned} \quad .$$

Once the unknown constants are resolved, the interpolation function is uniquely defined by the following seven parameters: t_{eivc}, α_{eivc}, $\dot{\alpha}_{eivc}$, t_{es}, t_{ee}, α_{ee} and τ.

The described activation function is used for ventricles and atria with a note that atrial contraction precedes ventricular contraction by time t_{av} (also known as PR interval in ECG). Panel A in Fig. 2 shows typical activation functions for ventricles (black line) and atria (blue line), and time derivative of ventricular activation function (red line). Here, we assume the same activation function for the left and for the right ventricle and the same activation function for the left and for the right atrium.

Numerical procedure

The mathematical model (the set of 24 ordinary differential equations) is integrated by the fourth order Runge-Kutta method. Initially, all flow rates are set at zero, and the volumes of all chambers set at values at the expected average pressure for each chamber. The integration is performed over multiple heart periods (usually ten periods is enough), in order to achieve cycle-to-cycle periodicity, and the results of the last cycle are taken. Integration time step was 1 ms.

Computational results and discussion

Typical results of the described model are presented in Fig. 2. The given results are for a normal subject with an arterial blood pressure of 120 / 80 mmHg, (green line in panel B). Left ventricular and atrial pressures are shown in black and blue line, respectively. There is no incisure in the arterial pressure wave form that is normally seen in invasively obtained measurements, because we did not model aortic valve dynamics. Panel C shows velocity profiles through the aortic valve (black line), mitral valve (blue line) and pulmonary veins (red line). Velocity peaks and profiles are in close agreement with the observations obtained by Doppler Echocardiography in normal subjects. In pulmonary veins flow we can see three distinct waves: positive S and D-wave as well as the negative A-wave. Panel D shows the time variation of left ventricular (black line) and atrial volume (blue line). It is visible that the range of change of atrial volume is much smaller than the ventricular one, since the atrium simultaneously fills and empties.

Fig. 3 shows pressure-volume loops for the left atrium (top panel) and ventricle (bottom panel). Pressure variation in the left atrium is within the physiological range and the shape of p-V loop correctly reflects events in the left atrium during one cycle. The same is valid for the left ventricle.

In the proposed formulation of heart systolic function (defined by Eqs. (7) to (9)) the needed parameters can be well estimated for each subject specifically, in subjects having mitral (and tricuspid) regurgitation. For this purpose, we use blood velocity profiles through the aortic (v_{av}) and mitral (v_{mv}) valve obtained by Doppler Echocardiography during systole. Since the opening in mitral valve during systole is small, the inertial effect and line friction losses are negligible ($M = 0$ and $R = 0$) and minor loss coefficient $K = 1$, it follows from Eq. (2) that

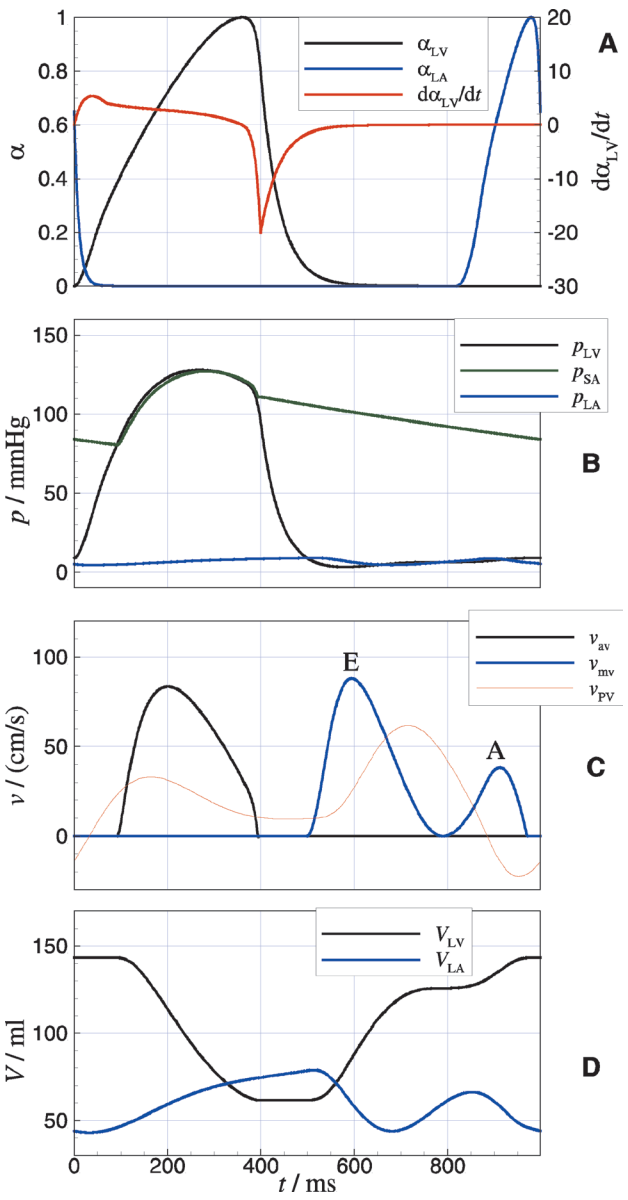

Fig. 2. Results from the proposed model. Panel A: activation function for ventricles and atria, and time derivative of left ventricular activation function; Panel B: Time variation of left ventricular, left atrial and systemic artery pressures; Panel C: time variation of aortic and mitral valve and pulmonary vein velocities; Panel D: Time variation of left ventricular and left atrial volume

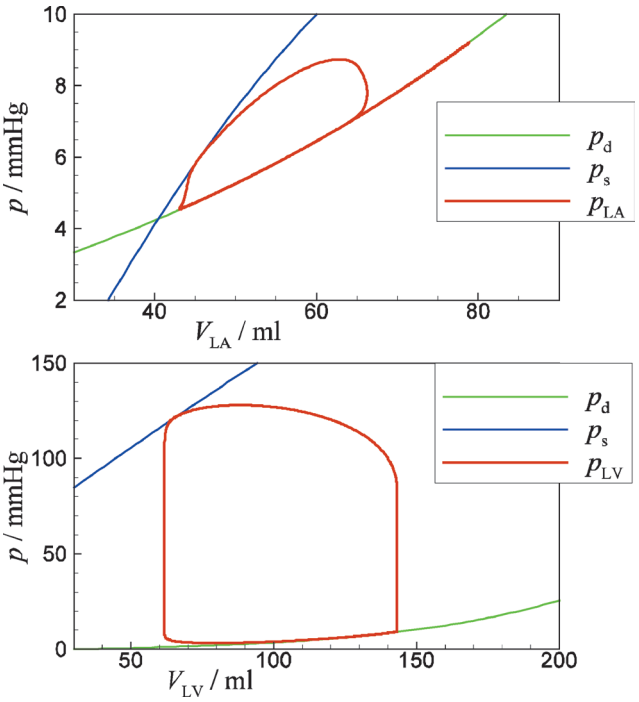

Fig. 3. Pressure-volume loop for left atrium (top) and left ventricle (bottom)

$$p_{LV} = p_{LA} + \frac{\rho}{2} v_{mv}^2 . \quad (10)$$

In Eq. (10) p_{LA} is small and can be either neglected or replaced by its average value. In Eq. (7) the passive pressure p_d is much smaller than p_s, and after neglecting it we have:

$$p_{LV} = \alpha(t) p_s(V_{LV}) . \quad (11)$$

We obtain the stroke volume by integration of v_{av} during the ejection time T_{ej}

$$V_{stroke} = \frac{D_{av}^2 \pi}{4} \int_0^{T_{ej}} v_{av} \, dt , \quad (12)$$

where D_{av} is the left ventricular outflow tract diameter, also measured by Doppler Echocardiography. End diastolic volume is $V_{ed} = V_{stroke} / E_f$, where E_f is the ejection fraction which can be estimated by the Teicholz echo method. The time variation of V_{LV} is then

$$V_{LV}(t) = V_{stroke} - \frac{D_{av}^2 \pi}{4} \int_0^t v_{av}(t') \, dt' . \quad (13)$$

For the given $\alpha(t)$ and V_{LV} we calculate p_s from Eq. (11) and find the coefficients in Eq. (8) by parabolic curve fitting.

There are seven parameters defining the activation function, and two of them (t_{eivc} and t_{ee}) are measured, t_{es} should be in the range defined by the time of the maximum p_{LV} and t_{ee}, and the rest four should satisfy some conditions at the end of isovolumic contraction and at the beginning of isovolumic relaxation. It follows from Eq. (11) that at constant V_{LV} it holds:

$$\frac{dp_{LV}}{dt} = p_s \frac{d\alpha}{dt} . \quad (14)$$

When we apply Eqs. (11) and (14) at $t = t_{eivc}$ when $V_{LV} = V_{ed}$ and $p_{LV} = p_{dia}$ (p_{dia} is the arterial diastolic pressure) and $t = t_{ee}$ when $V_{LV} = V_{es} = V_{ed} - V_{stroke}$ and $p_{LV} = p_{ee}$ (p_{ee} is the ventricular aortic valve closing pressure), we have

$$p_{dia} = \alpha_{eivc} p_s(V_{ed}) , \; p_{ee} = \alpha_{ee} p_s(V_{es}) ,$$
$$\left.\frac{dp_{LV}}{dt}\right|_{eivc} = p_s(V_{ed}) \dot{\alpha}_{eivc} \text{ and } \left.\frac{dp_{LV}}{dt}\right|_{ee} = p_s(V_{es}) \dot{\alpha}_{ee} . \quad (15)$$

If we accept exponential decay low for pressure and activation function, then we have two additional relations

$$\left.\frac{dp_{LV}}{dt}\right|_{ee} = \frac{p_{ee}}{\tau} \text{ and } \dot{\alpha}_{ee} = \frac{\alpha_{ee}}{\tau} . \quad (16)$$

Since we can estimate the left ventricular pressure and also its time derivative at $t = t_{eivc}$ and $t = t_{ee}$ from the mitral regurgitant flow, we use the above relations to find parameters defining activation function.

In the following paper we discuss the method of parameter estimation for pulmonary circulation.

There is still more room for improvements of the proposed model, since:

1) The model does not include valve dynamics. It is known that valve closing causes water hammer, i.e. incisure in the pressure profile.
2) Also, excursion of the annular planes of tricuspid and mitral valve may have an impact on the heart hemodynamic in different phases of cardiac cycle, so it would be of interest to include it into the model.
3) We use the four-element Windkessel model for the arterial systems. Windkessel models with more elements will represent the heart afterload more accurately.
4) Coupling of the lumped parameter model for the heart and one-dimensional model for arteries would provide more information of interest for clinicians.

References

[1] Mukkamala, R. A Cardiovascular Simulator for Research: User's Manual and Software Guide. 2004.

[2] Heldt T, Mukkamala R., Moody G.B., and Mark R.G., CV-Sim: An Open-Source Cardiovascular Simulator for Teaching and Research, Open Pacing Electrophysiol Ther J. 3: 45–54, 2010.

[3] Delhaas A.T., P., Verbeek B.X., and Prinzen F. W., Adaptation to mechanical load determines shape and properties of heart and circulation: the CircAdapt model. Am. J. Physiol. Heart Circ. Physiol. 288:H1943–H1954, 2005.

[4] Korakiantis T, Shi Y., A concentrated parameter model for human cardiovascular system including heart valves and atrioventricular interaction, Medical Engineering & Physics 28: 613-628, 2006.

[5] Müller L.O. and Toro E.F., A global multiscale mathematical model for the human circulation with emphasis on the venous system, Int. J. Numer. Meth. Biomed. Engng. DOI: 10.1002/cnm.2622, 2014.

[6] Broomé M., Maksuti E., Bjällmark A., FrencknerB., and Janerot-Sjöberg B., Closed-loop real-time simulation model of

hemodynamics and oxygen transport in the cardiovascular system, BioMedical Engineering OnLine 12:69, 2013.

[7] Suga H, Sagawa K, Shoukas AA, Load independence of the instantaneous pressure-volume ratio of the canine left ventricle and effects of epinephrine and heart rate on the ratio. Circulation Research. 32:3, 314-322, 1973.

[8] Raff GL, Glanz SA, Volume loading slows left ventricular isovolumic relaxation rate. Circ. Res. 48,813-824, 1981.

Fabijan Lulić[1], Zdravko Virag[2], Ivan Korade[2], Marko Jakopović[1]

Non-invasive Method for Parameter Identification in a Lumped Parameter Model of Pulmonary Circulation

[1] University of Zagreb, Pulmonary Disease Clinic
[2] University of Zagreb, Faculty of Mechanical Engineering and NavalArchitecture

Introduction

Understanding the function of the right heart and pulmonary circulation becomes more and more important in the treatment of cardiac and pulmonary diseases [1]. Hemodynamic data for examination of pulmonary circulation are usually obtained invasively, what is unacceptable in healthy subjects. That is why we need a non-invasive clinical method for the estimation of pulmonary circulation function that would be suitable for all subjects (with normal function and with cardiorespiratory diseases).

The aim of this work is to develop a lumped parameter model of pulmonary circulation and to develop a method for parameter identification of this model, based on non-invasive (Echocardiography) measurements of velocity profiles through heart valves.

Mathematical model

Fig. 1 schematically shows the right heart, pulmonary artery (PA), lungs, pulmonary veins (PV) and left atrium (LA) as well as the electrical analogue scheme of the proposed lumped model of pulmonary circulation. Resistor R models the total pulmonary vascular resistance, capacitors C and C_1 model arterial compliances of proximal and distal parts, L represents the inertial effects within arteries, η is the wall resistance of the proximal part (the Voigt model) and Z models the impedance of the rest of the system. For the given model parameters and for input pulmonary valve flow ($Q_{pv} = v_{pv} A_{pv}$), it is possible to calculate pulmonary root pressure (p_{PA}). When p_{PA} is measured, it is possible to find optimal values of model parameters which minimize the RMS error between measured p_{PA} and p_{PA} calculated with the model.

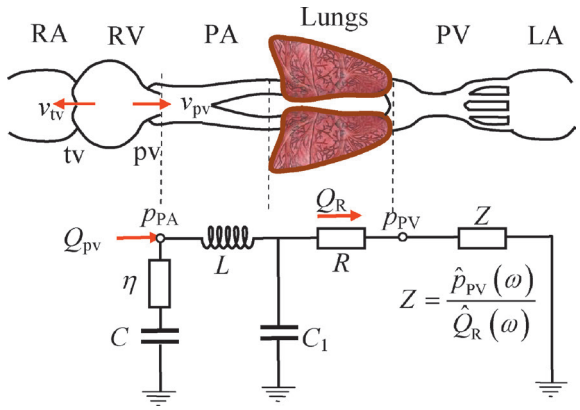

Fig. 1. Schematics of the pulmonary circulation and electrical analogue scheme of its lumped mathematical model. RA/RV = right atrium/ventricle, PA/PV = pulmonary arteries/veins, LA = left atrium, tv/pv = tricuspid/pulmonary valve, Z = impedance, ω = circular frequency

Measurements

By using Doppler Echocardiography, it is possible to measure pulmonary valve (v_{pv}) and tricuspid regurgitant blood velocity (v_{tv}). In each particular case, several measurements were recorded and the average data profiles were calculated. The "measured" p_{PA} is obtained from unsteady Bernoulli equation

$$p_{PA} = p_{RA} + \frac{1}{2}\rho v_{tv}^2 - \frac{1}{2}K\rho v_{pv}^2 - \rho l \frac{dv_{pv}}{dt}, \qquad (1)$$

where K and l are minor loss coefficient and inertial length through the pulmonary valve, respectively, p_{RA} is the average right atrium pressure, which is estimated from the width of vena cava inferior. Similarly, the average pressure in pulmonary veins (p_{PV}) is estimated from the mitral inflow pattern. The stroke volume calculated from the pulmonary and aortic valve velocity should be the same

$$V_{stroke} = \int_0^{T_{ej}} v_{pv} A_{pv} dt = \int_0^{T_{ej}} v_{av} A_{av} dt, \qquad (2)$$

where T_{ej} is ejection time. Since the aortic valve area can be measured more precisely, we use Eq. (2) to calculate A_{pv}.

Parameter identification

First, the pulmonary artery input impedance $Z_{in} = \hat{p}_{PA}/\hat{Q}_{pv}$ (the ratio of the pressure and flow phasors defined by the Fourier series) is calculated, and then p_{PA}^{WK5} is obtained based on measured Q_{pv}. This pressure is compared with the p_{PA} defined by Eq. (1), and the error defined as

$$RMSE = \sqrt{\frac{1}{N}\sum_{i=1}^{N}\left(p_{PA}^{WK5} - p_{PA}\right)^2} \qquad (3)$$

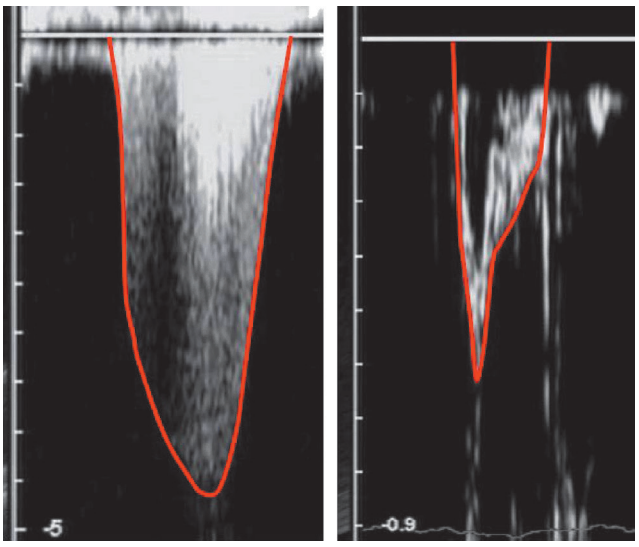

Fig. 2. Example of Doppler regurgitant tricuspid (left) and pulmonary velocity (right). Red lines are plotted for a digitization purpose

(where N is the number of points within T_{ej}) is minimized.

Results and Remarks

The method was applied to an elderly patient with pulmonary arterial hypertension using the following data: Cardiac Output: 5 l/min, Heart Rate 78 beat/min, pulmonary valve diameter D_{pv} = 2.73 cm, isovolumic contraction of RV time t_{eivc} = 34.4 ms, p_{RA} = 5 mmHg, p_{PV} = 10 mmHg, $l = 1.53D_{pv}$, $K = 1$. Fig. 3 shows the measured pulmonary flow, and the comparison of the measured and calculated pressure during T_{ej}. p_{PA}^{WK5} from the model describes the "measured" pressure very well, and shows incisure immediately after pulmonary valve closing. Fig. 4 shows the pulmonary input impedance and the values of model parameters that minimize RMSE. The absolute value of Z_{in} shows its minimum value and zero crossing frequency of the phase angle is 5.4 Hz, what is in good agreement with the observations of elderly subjects.

The proposed method is capable to accurately identify PA model parameters and input impedance of pulmonary circulation by using the pressure data from the ejection time window only.

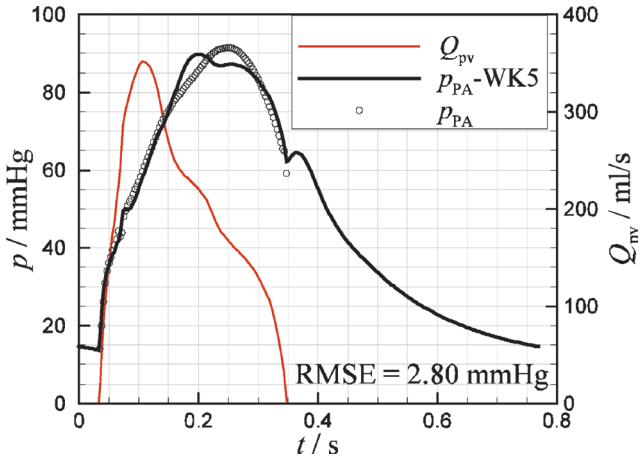

Fig. 3. Velocity through the pulmonary valve (thin red line), "measured" pulmonary root pressure from Eq. (1) (circles), and pulmonary root pressure from the five element lumped model (thick black line)

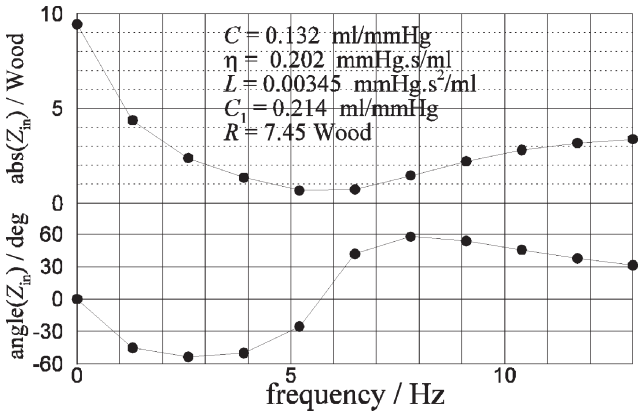

Fig. 4. Absolute value of pulmonary input impedance (upper part) and its phase angle (lower part)

The method is limited to the subject with nicely obtainable tricuspid regurgitant velocity and pulmonary valve flow.

References

[1] Peacock, A.J., Naeije, R., Rubin, L.J., Pulmonary circulation: Diseases and their Treatment. Hodder Arnold, 3rd ed., 2011.

Zdravko Virag[1], Fabijan Lulić[2], Severino Krizmanić[1]

Mathematical Model of Blood Flow Through the Aortic Valve

[1] University of Zagreb, Faculty of Mechanical Engineering and Naval Architecture,
[2] University of Zagreb, Pulmonary Disease Clinic

Introduction

In lumped models of circulatory system the aortic flow is governed by unsteady Bernoulli equation. The aortic valve is usually considered as the idealized check valve. This means that the valve opens instantaneously for the positive flow and closes instantaneously preventing the negative (reverse) flow from arteries to the left ventricle. The invasive measurements show that during the valve closing phase the negative flow always occurs. The negative flow cannot be obtained by the idealized valve model. Here we have proposed a model of the aortic valve that could also predict the negative aortic flow.

Mathematical model and numerical method

The characteristic opening and closing phases of the aortic valve are shown in Fig.1. Initially (at the beginning of systole) there is no blood flow through the aortic valve, and the valve leaflets are at rest (panel A in Fig. 1). When the left ventricle (LV) pressure exceeds the arterial pressure (due to LV contraction), the unsteady Bernoulli equation holds

$$M\frac{\mathrm{d}Q}{\mathrm{d}t} = p_{\mathrm{lv}}^{M} - p_{\mathrm{sa}}^{\mathrm{M}} - \frac{K\rho}{2A_{\mathrm{av}}^2}\left(Q - Q_{\mathrm{L}}\right)^2, \qquad (1)$$

where Q is the absolute blood flow through the aortic root, M is inertance coefficient, $\rho = 1050$ kg/m^3 is blood density, A_{av} is the aortic root area, $p_{\mathrm{lv}}^{\mathrm{M}}$ and $p_{\mathrm{sa}}^{\mathrm{M}}$ are measured left ventricle and arterial pressure, respectively, K is minor loss coefficient and Q_{L} is the flow rate that defines the volume V_{L} swept by valve leaflets

$$\frac{\mathrm{d}V_{\mathrm{L}}}{\mathrm{d}t} = Q_{\mathrm{L}}. \qquad (2)$$

During the first opening phase, leaflets move into the arterial space with $Q_{\mathrm{L}} = Q$, but there is no orifice. The orifice occurs after the leaflets have swept a certain volume (see panel B in Fig. 1) $V_{\mathrm{L0}} = \alpha A_{\mathrm{av}}\sqrt{4A_{\mathrm{av}}/\pi}$, where α is the model parameter. During the second opening phase the orifice increases from zero to A_{av}, and leaflets sweep an additional volume (see panel C in Fig. 1) $V_{\mathrm{L1}} = \beta A_{\mathrm{av}}\sqrt{4A_{\mathrm{av}}/\pi}$, where β is the model parameter. In this phase $Q_{\mathrm{L}} = \left(1 - A/A_{\mathrm{av}}\right)Q$, where A is the orifice area which is related to V_{L} as $A = \left[\left(V_{\mathrm{L}} - V_{\mathrm{L0}}\right)/V_{\mathrm{L1}}\right]^2$, see [1]. During these two phases the inertance coefficient is defined as $M = \left(2 - A/A_{\mathrm{av}}\right)M_0$, where $M_0 = \rho L/A_{\mathrm{av}}$ and L is inertance length. After the flow has reached its maximum, the slow leaflets closing phase starts with $Q_{\mathrm{L}} = Q - Q_{\max}A/A_{\mathrm{av}}$. During this phase V_{L} decreases from $V_{\mathrm{L0}} + V_{\mathrm{L1}}$ to V_{L0} (see panels D and E in Fig. 1), and at a certain moment Q becomes negative. For negative Q the inertance coefficients is defined as $M = \delta M_0$, where δ is model parameter. At the end of this phase (for $V_{\mathrm{L}} = V_{\mathrm{L0}}$, see panel E in Fig. 1) leaflets coapt and equation (1) does not hold anymore. Measurements suggest that in the last rapid closing phase (after the leaflets coapt) the leaflets behave as a dumped oscillating system defined by

$$\frac{\mathrm{d}^2Q}{\mathrm{d}t^2} + 2\xi\frac{\mathrm{d}Q}{\mathrm{d}t} + (\omega^2 + \xi^2)Q = 0, \qquad (3)$$

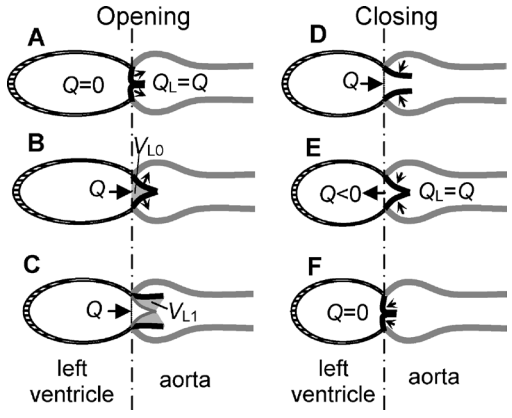

Fig. 1. Scheme of aortic valve opening (panels A to C) and closing (panels D to F)

where ξ and ω are constant parameters. During this phase $Q_{\mathrm{L}} = Q$, and V_{L} should decrease from V_{L0} to zero. If we introduce another parameter $\gamma = \xi/\omega$, parameters ξ and ω are uniquely defined by V_{L0} (or α) and γ.

For the given measured left ventricular and arterial pressures and the set of model parameters: A_{av}, L, K, α, β, γ and δ, the set of equation (1) or (3) and (2) is solved numerically by the fourth order Runge-Kutta method.

Results and conclusions

The proposed model was applied to the measured data in humans and pigs. The measured left ventricle and arterial pressure was used as input, and the calculated aortic flow was compared with the measured ones in Figs. 2 and 3.

There is a very good agreement of the model results with the measured ones, with model parameters in physiological range. Time varying aortic valve orifice A shows two closing phases: a slow one followed by a rapid one as it

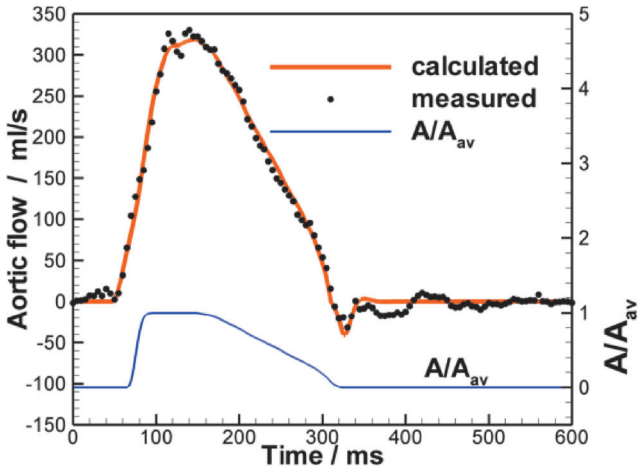

Fig. 2. Model results and measured data [2] in human (model data were $A_{\mathrm{av}} = 2.9$ cm^2, $L = 3$ cm, $K = 1$, $\alpha = 0.15$, $\beta = 0.4$, $\gamma = 0.8$, $\delta = 10$)

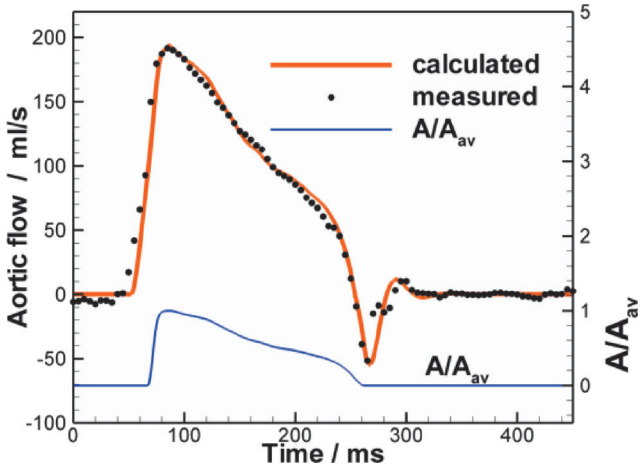

Fig. 3. Model results and measured data [3] in pig (model data were $A_{\mathrm{av}} = 1.6$ cm^2, $L = 1$ cm, $K = 1$, $\alpha = 0.5$, $\beta = 0.6$, $\gamma = 0.5$, $\delta = 3$)

is in experimental observations. The model indicates that the leaflets coapt before the maximal back-flow occurs.

References

[1] Z. Virag and F. Lulić, Modeling of aortic valve dynamics in a lumped parameter model of left ventricular-arterial coupling: Ann. Univ. Ferrara, Vol 54 (2008) 335-347.

[2] RP Kelly, CT Ting, TM Yang, CP Liu, WL Maughan, MS Chang and DA Kass, Effective arterial elastance as index of arterial vascular load in humans: Circulation, Vol 86 (1992) 513-521.

[3] P. Segers, N. Stergiopulos, N. Westerhof, P. Wouters, P. Kolh and P. Verdonck, Systemic and pulmonary hemodynamics assessed with a lumped-parameter heart-arterial interaction: J. of Eng. Math., Vol 47, 3-4 (2003) 185-199.

Zdravko Virag[1], Fabijan Lulić[2]

Application of Three Lumped Models of the Arterial Tree to Subjects of Different Age

[1] University of Zagreb, Faculty of Mechanical Engineering and Naval Architecture
[2] University of Zagreb, Pulmonary Disease Clinic

Introduction

The arterial tree is a network of visco-elastic blood vessels, which delivers blood to the whole body. The simplest models of the arterial tree are lumped models, which describe the arterial tree as one or several compliant chambers. The lumped models are attractive for clinicians because they describe the function of the whole arterial tree in terms of simple parameters such as compliance, resistance, and inertance [1]. The main purpose of lumped parameter models is to model the arterial input impedance (the pressure-to-flow ratio in the frequency domain: $Z = p / Q$) as an afterload to the left ventricle. Lumped models are also used to define the total arterial compliance and resistance, which can explain changes in arterial trees due to ageing and diseases.

The goal of this work was to estimate the capability of different lumped models to properly reconstruct arterial tree pressure from the arterial valve flow. We defined three lumped models of the arterial tree: with one, two and three chambers. The models were applied to three typical subjects of different age (adolescent, middle-aged and elderly).

Materials and methods

Fig. 1 shows the measured aortic root pressure and aortic valve flow for the three typical subjects of different age [2].

One-dimensional models of the arterial tree are governed by partial differential equations, which are usually solved numerically. In a numerical procedure the arterial tree is divided into a number of short elements of different diameter and wall properties. In the case of the Voigt model for the arterial wall, each element can be considered as a chamber defined by the compliance and wall resistance (viscosity), while inertance and resistance characterize the flow along the chambers. By reducing the number of elements in a one-dimensional model to one or a few, a lumped model is obtained. Such reduction from one-dimensional to the lumped model is appropriate when the wave speed tends to infinity [3] (in real problems when the product of wave speed and heart period is much greater than the length of the aorta).

Here we used three lumped parameter (or Windkessel) models consisting of one, two and three chambers, which are defined by three (WK3), six (WK6) and nine (WK9) parameters, respectively. Fig. 2 shows the electrical analogue schemes of the selected Winkessel models. In the WK3 model (also called viscous Windkessel [4]) C_0 and η_0 define the visco-elastic chamber and R represents the peripheral resistance. It is clear that the one-chamber Windkessel model cannot describe any travel or reflection of pressure wave. That is why we chose WK6 and WK9 models, which consist of two and three chambers, respectively. The WK6 model is an extended five element model [5] (extension is resistance r_1), while the WK9 model can be considered as a step toward the one-dimensional model, and it is not used in literature, probably because it contains too many parameters for a lumped model. In a Windkessel model with at least two chambers there is a mass redistribution between chambers and such a model can mimic elementary pressure wave reflection. For example, in the WK6 model a visco-elastic chamber (defined by C_0 and η_0

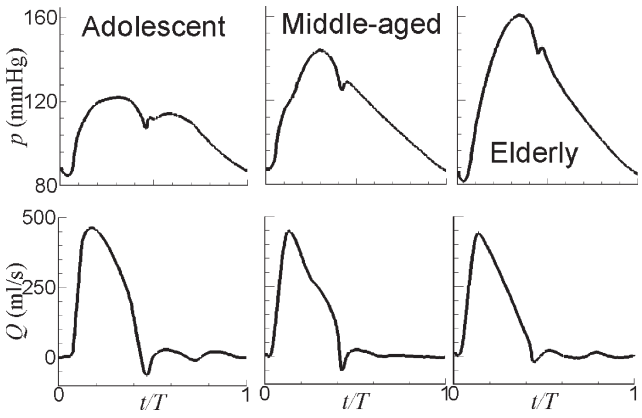

Fig. 1. Recorded aortic root pressure (top) and aortic valve flow (bottom down) for three subjects of different age (T is heart period)

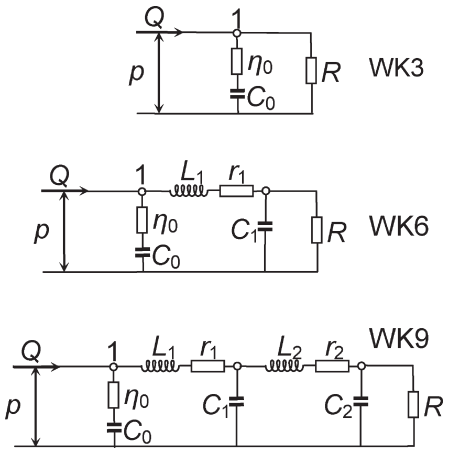

Fig. 2. Electrical analogue schemes of the selected lumped models of the arterial tree

as in the WK3 model) is connected by inertance L_1 and resistance r_1 with the other, purely elastic chamber (defined by C_1). Peripheral resistance R has a similar meaning as in the case of the WK3 model. Unfortunately, there is no unambiguous explanation what these two chambers in the WK6 model represent. They can be two parts of large arteries or the first chamber can represent large arteries, while the second one represents small arteries. The same applies to the WK9 model.

The measured aortic valve flow is applied at the inlet (at point 1 in Fig. 2). The input pressure is calculated by using the model. The model parameters are obtained by minimizing the pressure root mean squared error (RMSE) defined as

$$\mathrm{RMSE} = \sqrt{\sum_1^n \left(p - p^{\mathrm{calc}}\right)^2 / n}\,, \qquad (1)$$

where p^{calc} and p are the calculated and the measured aortic root pressure, respectively, and n is the number of time instants during the heart period at which the pressure is measured.

In the cases of the WK6 and the WK9 models, there are several local minima, and the solution depends on the starting point. To increase a chance to find the point with the absolute RMSE minimum we calculated the RMSE at a number of randomly selected points within the parameter domain, and for the starting point, we chose the one with the minimal RMSE.

Results and Discussion

The model parameters are identified from the measured data for three subjects (Fig. 1). Table 1 shows the values of the obtained parameters for all models and the achieved RMSE values. Fig. 3 illustrates the ability of the models to reconstruct the measured pressure from the measured flow, as well as the comparison between the measured and calculated input impedance.

Table 1 shows that the arterial compliance C_0 decreases with ageing (according to all models) and peripheral resistance increases. Because of reduced compliance the wave speed increases, and a Windkessel model becomes more appropriate [6]. This is an explanation why the WK3 model reconstructs the measured pressure better (with lower RMSE) in the case of the elderly subject than in the case of the middle-aged or the adolescent one. In the case of the adolescent subject, the wave speed is low and the pressure wave reflection at the aortic root occurs during diastole (see the secondary pressure rise in Fig. 1), when the aortic valve flow is equal to zero. The WK3 model cannot describe such phenomena and a Windkessel model with more chambers (or even better a one-dimensional model) is required. Table

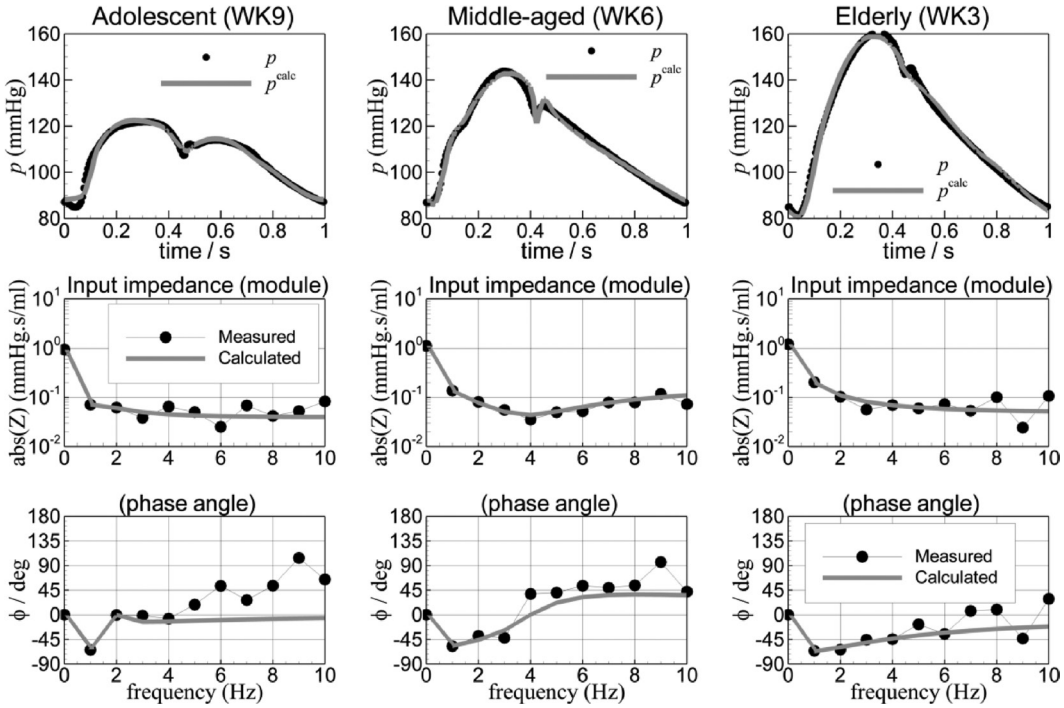

Fig. 3. Measured and calculated pressure for the three subjects and the measured and the calculated input impedance (modulus and phase angle)

Table 1. The obtained values of the model parameters for three subjects (C_0, C_1 and C_2 are expressed in ml/mmHg; η_0, r_1, r_2 and R in mmHg·s/ml; L_1 and L_2 are in mmHg·s²/ml; RMSE is in mmHg)

Subject:	Adolescent			Middle-aged			Elderly		
Model:	WK3	WK6	WK9	WK3	WK6	WK9	WK3	WK6	WK9
C0	2.538	1.708	2.213	1.239	0.738	0.624	0.769	0.412	0.202
10η0	0.401	0.423	0.393	0.617	1.853	2.075	0.504	1.199	0.702
1000L1		19.49	8.638		2.848	3.070		2.360	1.512
10r1		0.000	0.146		0.516	0.375		0.630	0.637
C1		0.436	2.965		0.593	0.579		0.383	0.661
1000L2			13.85			43.86			113.6
10r2			0.000			0.000			0.992
C2			5.584			0.107			0.096
R	0.908	0.908	0.893	1.116	1.064	1.078	1.202	1.139	1.039
RMSE	4.00	1.89	1.52	2.73	1.52	1.21	1.57	1.22	0.84

1 shows that the level of RMSE of less than 1.6 mmHg is obtained for the adolescent subject by the WK9 model, for the middle-aged subject by the WK6 model and for the elderly subject by the WK3 model. The one chamber model is appropriate for the arterial tree of older subjects (with stiffer aorta), and in the case of younger subjects, a lumped model with two or three chambers is a better choice.

References

[1] Westerhof N., Lankhaar JW., Westerhof B.E.: The arterial Windkessel. Med. Biol. Eng. Comput. (2009) 47:131–141.

[2] Nichols W.W., O'Rourke M.F.: McDonald's Blood flow in Arteries. Theoretical, experimental and clinical principles, (2005) 5th ed., Arnold, London.

[3] Christopher C. M., Berger D. S., Noordergraaf A.: Apparent arterial compliance, Am. J. Physiol. 274 (Heart Circ. Physiol. 43): H1393–H1403, 1998.

[4] Burattini R., Natalucci S.: Complex and frequency-dependent compliance of viscoelastic windkessel resolves contradictions in elastic windkessels, Medical Engineering & Physics 20, 502–514, 1998.

[5] Toy S. M., Melbin. J., Noordergraaf A.: Reduced Models of Arterial Systems, IEEE Transactions on Biomedical Engineering, Vol. BME-32, No. 2, 174-176, and 1985.

[6] Mohiuddin M. W., Laine G. A., Quick C. M.: Increase in pulse wavelength causes the systemic arterial tree to degenerate into a classical windkessel, Am J Physiol Heart Circ Physiol 293: H1164–H1171, 2007.

Ivan Korade, Zdravko Virag and Mario Šavar

Numerical Simulation of One-dimensional Blood Flow in Elastic and Viscoelastic Arterial Network

University of Zagreb, Faculty of Mechanical Engineering and Naval Architecture

Introduction

Numerical simulation of blood flow in the arterial tree is challenging due to difficulties in describing the gemetry, nonlinear wall viscoelasticity, and non-Newtonian rheological properties of blood. One-dimensional models present a good compromise between Windkessel and three-dimensional models [1, 2]. Numerical simulation of arterial flow is very useful for the thorough understanding of pressure and flow waves propagation phenomena.

The goal of this paper is to present a method of characteristics (MOC) [3, 4] for solving a nonlinear one-dimensional model in an arterial tree with elastic and viscoelastic wall. The developed method was applied to the 37-element silicone model of arterial tree with available experimental data [5]. The test was used in [6] to check the ability of the mathematical model and the numerical scheme of correctly describing the multiple reflections from multiple outflow and junction conditions. Here we used this benchmark to verify the in-house developed code by comparing the obtained results with the experimental data and with the results of other methods.

Mathematical model

A one-dimensional model of blood flow in a pipe with viscoelastic wall reads [6]:

$$\frac{\partial A}{\partial t}+\frac{\partial Q}{\partial x}=0\,, \tag{1}$$

$$\frac{\partial Q}{\partial t}+\frac{A}{\rho}\frac{\partial p}{\partial x}+\frac{\partial (Qv)}{\partial x}=-fQ\,, \tag{2}$$

$$p - p_0 = \frac{1}{C_D}(\sqrt{A} - \sqrt{A_0}) + \eta \frac{\partial A}{\partial t}, \qquad (3)$$

where x, t are the space and the time coordinate, respectively, A is cross-sectional area ($A = D^2\pi/4$), Q is volume flow rate, and $v = Q/A$, p is transmural pressure, ρ is fluid density, A_0 is constant cross-sectional area at a constant pressure of p_0. Coefficients f, C_D and η are defined by:

$$f = \frac{2(\zeta+2)\pi\mu}{\rho A}, \quad C_D = \frac{3A_0}{4\sqrt{\pi}E\delta} \text{ and } \eta = \frac{\tau}{2C_D\sqrt{A}}, \qquad (4)$$

where μ is fluid viscosity, ζ is constant for particular velocity profile, E is elastic modulus and τ is retardation time constant in the Voigt model.

Numerical method

The artery is discretized into a number of elements of length Δx. Fig. 1 shows two typical elements (denoted by j and k) bounded by nodes (I, J, and K). The pressure is defined at the nodes, A is defined in the middle of each element (and it is considered to be constant along the element) and Q is defined at each end of each element. Thus, four unknowns are stored for each element. For example, the unknowns related to the element j are p_J, Q_{jL}, Q_{jD} and A_j, as shown in Fig. 1.

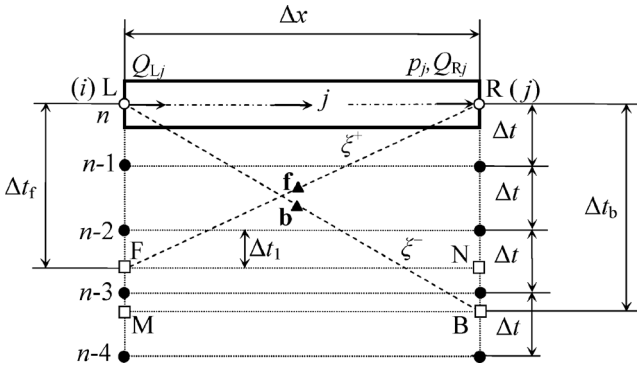

Fig. 1. An element of a discretized arterial tree with the arrangement of variables. For each element, three variables are stored: pressure p_j, flow rate Q_{Rj} at the element outlet, and Q_{Lj} at the element inlet. The time instances are denoted by n, n-1, n-2, n-3, and n-4. Dashed lines denote the characteristics defined by $\xi^+ = v + c$ and $\xi^- = v - c$; empty circles denote the nodes at the new instance at which unknowns should be calculated; filled circles denote nodes at older time instances at which the values of all variables are known from the previous integration steps; squares denote the interpolation points F and B on the forward and backward characteristic lines, and the auxiliary interpolation points N and M are at the same time instances as the points F and B, respectively; triangles denote midpoints f and b of the forward and backward characteristics, respectively

By using Eq. (3), Eqs. (1) and (2) can be transformed into a set of compatibility equations, which are valid along two characteristic lines defined by $\xi^{\pm} = v \pm c$ in the form:

$$\frac{1}{C}\mathrm{d}Q^{\pm} - (v \mp c)\,\mathrm{d}p^{\pm} = -\frac{1}{C} f Q \mathrm{d}t - v^2 \eta \frac{\partial^2 A}{\partial x \partial t}\mathrm{d}t + (v \mp c)\eta \frac{\partial^2 Q}{\partial x \partial t}\mathrm{d}t, \qquad (5)$$

where $C = 2C_D\sqrt{A}$, and $c = \sqrt{A/(\rho C)}$ is wave speed. We establish relationship between pressure and area from the discretized form of Eq. (3), which serves to exclude A from the set of unknowns. The third equation related to each node is the continuity equation. For example, at node R in Fig. 2, this equation reads:

$$Q_{Rj} = Q_{Wj} + \sum_{k=1}^{N_{out}} Q_{Lk}, \qquad (6)$$

where Q_{TJ} is the branching flow from the large artery into a small one, which is modeled by the inertial four element Windkessel as depicted in Fig. 2. In this model, L_J is inertance, r_J is resistance, C_{TJ} is the capacity of branching arteries and R_J is the peripheral resistance at node J.

We discretized Eq. (5) and all other auxiliary equations by using second order accuracy, and the resulting system of algebraic equation is solved by a direct method. The

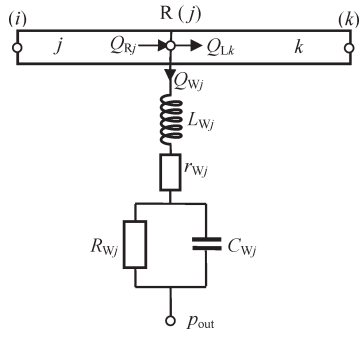

Fig. 2. Electrical analogue scheme of the Windkessel model defining the node outlet boundary condition

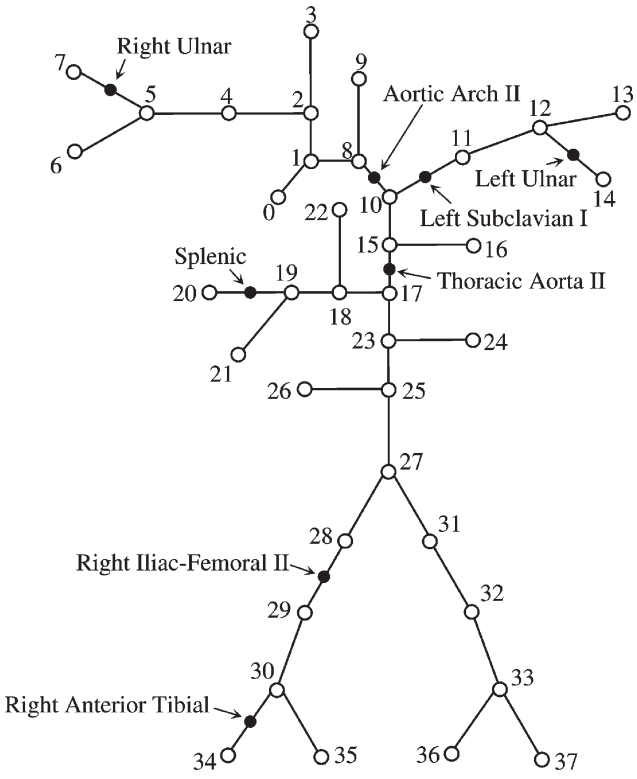

Fig. 3. Scheme of 37-segment arterial tree. The node number zero denotes the arterial tree inlet, where a periodic flow rate was prescribed. Filled circles denote measurement sites

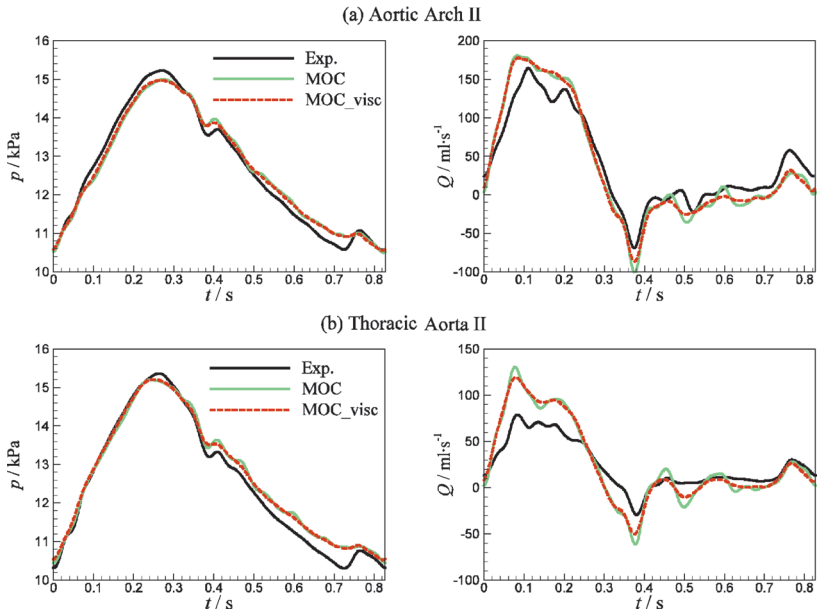

Fig. 4. 37-artery network. Pressure (left) and flow rate (right) at midpoints of two arterial segments: (a) Aortic Arch II and (b) Thoracic Aorta II. Black solid lines represent in vitro experimental data (Exp.), green solid lines denote numerical results of the developed method with elastic arterial wall (MOC), and red dashed lines denote numerical results of the method of characteristics with viscoelastic arterial wall (MOC_visc) [4]

Table 1. Percentage RMS errors of the calculated pressure and flow rate with respect to the measurements at the locations indicated in Fig. 3, and the range of these errors from six other numerical schemes

Arterial segment	Numerical scheme		ε_p^{RMS}	ε_Q^{RMS}
Aortic arch II	Six schemes	min	1.68	12.02
		max	1.94	12.34
	MOC		1.77	12.47
	MOC – visc.		1.56	11.89
Thoracic aorta II	Six schemes	min	2.17	25.26
		max	2.53	25.62
	MOC		2.26	26.27
	MOC – visc.		2.15	24.50
Left subcl. I	Six schemes	min	3.05	13.87
		max	3.12	14.45
	MOC		3.19	14.39
	MOC – visc.		3.04	13.53
R. iliac-femoral II	Six schemes	min	3.65	23.90
		max	3.97	24.80
	MOC		3.97	26.02
	MOC – visc.		3.68	22.52
Left ulnar	Six schemes	min	2.57	12.42
		max	2.75	12.91
	MOC		2.67	12.81
	MOC – visc.		2.28	11.36
R. anter. tibial	Six schemes	min	3.21	9.88
		max	3.43	11.05
	MOC		3.90	10.98
	MOC – visc.		3.15	8.15
Right ulnar	Six schemes	min	2.42	11.22
		max	2.66	11.73
	MOC		2.62	11.84
	MOC – visc.		2.53	10.70
Splenic	Six schemes	min	2.22	9.02
		max	2.36	9.79
	MOC		2.52	10.37
	MOC – visc.		1.93	7.80

method is implicit, unconditionally stable and capable of dealing with nonlinearities.

At the inlet node the pressure or the inflow can be prescribed. In all simulations, the initial conditions were $Q(x,0)=0$, $A(x,0)=A_0$ and $p(x,0)=p_0$. The integration time should be long enough to achieve cycle-to-cycle periodicity, and the last cycle is examined.

Results and discussion

Fig. 3 schematically shows the examined network. All data relevant to this problem are provided in the supplement material [6]. In the performed simulation each segment was divided into a number of elements (total number of elements was 431), and integration time step was 1 ms. Fig. 4 shows the comparison of the measured and calculated pressure and flow (for the case of elastic and viscoelastic wall), and Table 1 shows the percentage root mean square (RMS) errors of the calculated results with respect to the experimental data of the developed method and the range of these errors from the six other methods examined in [6].

In the case of elastic wall, most of the MOC errors are very similar in size to errors from six numerical schemes (see Table 1). In the case of viscoelastic wall, the pressure and flow RMS errors are slightly reduced, and a reduction in peak values of pressure and flow rate is achieved (that is closer to experimental data) because of damping high frequency oscillations.

References

[1] Ottesen, JT, Olufsen, MS, Larsen, JK. *Applied mathematical models in human physiology*. SIAM: Society for Industrial and Applied Mathematics, 2004.

[2] van de Vosse FN, Stergiopulos N. Pulse wave propagation in the arterial tree. *Annual Review of Fluid Mechanics* 2011; **43**(1): 467–499. DOI: 10.1146/annurev-fluid-122109-160730.

[3] Korade I, Virag Z, Šavar M. Numerical simulation of one-dimensional flow in elastic and viscoelastic branching tube. *Proceedings of the 6th European Conference of Computational Fluid Dynamics (ECFD VI)*, Oñate E, Oliver X, Huerta A (ur). International Center for Numerical Methods in Engineering (CIMNE): Barcelona, Spain, July 20-25, 2014; 7124–7131.

[4] Korade I, Modeliranje strujanja krvi u arterijskom stablu s viskoelastičnom stijenkom (eng. Modeling of Blood Flow in an Arterial Tree with Viscoelastic Wall), PhD, University of Zagreb, Faculty of Mechanical Engineering and Naval Architecture, 2017.

[5] Matthys KS, Alastruey J, Peiró J, Khir AW, Segers P, Verdonck PR, Parker KH, Sherwin SJ. Pulse wave propagation in a model human arterial network: Assessment of 1-D numerical simulations against in vitro measurements. *Journal of Biomechanics* 2007; 40 (15):3476–3486. doi:10.1016/j.jbiomech.2007.05.027.

[6] Boileau E, Nithiarasu P, Blanco PJ, Müller LO, Fossan FE, Hellevik LR, Donders WP, Huberts W, Willemet M, Alastruey J. A benchmark study of numerical schemes for one-dimensional arterial blood flow modelling. *International Journal for Numerical Methods in Biomedical Engineering* 2015; 31(10):e02732 (33 pages). doi:10.1002/cnm2732.

Ivan Korade[1], Zdravko Virag[1], Fabijan Lulić[2]

Estimation of Velocity Profile and Pulsatile Wall Shear Stress in Arteries Using the Measured Maximal Velocity

[1] University of Zagreb, Faculty of Mechanical Engineering and Naval Architecture
[2] University of Zagreb, Pulmonary Diseases Clinic

Introduction

Blood flow in the arterial tree is essentially pulsatile. Time variation of the maximal velocity at certain points of the arterial tree may be obtained non-invasively and used for tuning of 1D model parameters. In 1D models it is convenient to assume a nearly flat velocity profile (blood flow rate is calculated as the product of maximal velocity and area) and Hagen-Poiseuille friction model derived from a steady state flow condition. The goal of this work was to estimate how good these two assumptions are. We used the measured maximal velocity and the Womersley quasi two dimensional (Q2D) solution of pulsatile flow in a rigid pipe [1] to define the velocity profile at the observed cross-section. From this velocity profile, the actual flow rate (or mean axial velocity) and wall shear stress were calculated.

Womersley solution of Q2D flow

We observed an incompressible fluid flow in a rigid circular pipe of radius *R* under a harmonic pressure gradient defined as:

$$\frac{\mathrm{d}p}{\mathrm{d}x} = S\sin(\omega t) + C\cos(\omega t), \tag{1}$$

where $p(x,t)$ is pressure, x is space coordinate along the pipe axis, t is time and ω is circular frequency. If we assume an axial velocity $u(r,t)$, the linear momentum equation is:

$$\rho\frac{\partial u}{\partial t} = \mu\left(\frac{1}{r}\frac{\partial u}{\partial r} + \frac{\partial^2 u}{\partial r^2}\right) - \frac{\mathrm{d}p}{\mathrm{d}x}, \tag{2}$$

where ρ is fluid density, μ is viscosity and r is radial coordinate. Eq. (2) is solved in the frequency domain, where the pressure gradient and axial velocity can be represented as real parts of:

$$\frac{\mathrm{d}p}{\mathrm{d}x} = \mathcal{R}e\left\{-i\hat{P}e^{i\omega t}\right\},\ u = \mathcal{R}e\left\{-i\hat{U}(r)e^{i\omega t}\right\}, \tag{3}$$

where $\hat{P} = S + iC$, and $\hat{U} = S_u + iC_u$ are complex amplitudes. The solutions for axial velocity, flow rate $Q = \int_0^R 2\pi u r \mathrm{d}r$ and wall shear stress τ_w are:

$$u = \mathcal{R}e\left\{\frac{\hat{P}}{\rho\omega}\left[1 - \frac{J_0(\Lambda y)}{J_0(\Lambda)}\right]e^{i\omega t}\right\}, \tag{4}$$

$$Q = \mathcal{R}e\left\{ i\frac{2\pi\hat{P}\mu}{\rho^2\omega^2}\left[-\frac{\mathrm{Wo}^2 i}{2} - \frac{\Lambda J_1(\Lambda)}{J_0(\Lambda)} \right] e^{i\omega t} \right\}, \quad (5)$$

$$\tau_w = \mathcal{R}e\left\{ \hat{P}\sqrt{\frac{\mu}{\rho\omega}}\frac{J_1(\Lambda)}{J_0(\Lambda)} e^{i\left(\omega t + \frac{3\pi}{4}\right)} \right\}, \quad (6)$$

where $\mathrm{Wo} = R\sqrt{\rho\omega/\mu}$ is Womersley number, $y = r/R$, $\Lambda = \mathrm{Wo}\,\exp(3\pi i/4)$, J_0 and J_1 are Bessel functions of the first kind and of zero and first order, respectively.

Method

The maximal velocity is defined by Eq. (4) for $y = 0$. We start from the measured maximal velocity $u^{\mathrm{M}}_{\max}(t)$ during one heart period T which may be decomposed into Fourier series:

$$u_{\max}(t) = \sum_{n=0}^{N}\left(S_u^n \sin(n\omega_0 t) + C_u^n \cos(n\omega_0 t) \right), \quad (7)$$

where $\omega_0 = 2\pi/T$, and N is the number of harmonics. Using Eq. (4) for $u_{\max}$, it is possible to calculate the complex pressure gradient amplitudes at each frequency $\omega = n\omega_0$, and after that to calculate $Q(t)$ and $\tau_w(t)$ from Eqs. (5) and (6) (as a sum of contributions of all N harmonics). The obtained average velocity $u_{\mathrm{avg}} = Q(t)/(R^2\pi)$ will be compared with the measured maximal velocity, and obtained $\tau_w(t)$ with $\tau_{w,\mathrm{S}} = 4\mu Q/(R^3\pi)$ obtained from the Hagen-Poiseuille formula.

Results

Simultaneous measurements of pressure gradient and axial velocity $u^{\mathrm{M}}(y,t)$ at $y =$ (0; 0.5; 0.75 and 0.95) in the femoral artery of a dog are given in [2]. We use $u^{\mathrm{M}}_{\max}(t) = u^{\mathrm{M}}(0,t)$ to calculate pressure gradient and axial velocity at the other measurement locations. The assumed Womersley number associated with the heart frequency is $\mathrm{Wo} = 3.8$. To check the applicability of the proposed method, we compared measured and reconstructed values depicted in Fig. 1.

Our results indicate that the proposed method could be used to estimate the axial velocity profile on the basis of the measured maximal velocity. Fig. 2 shows the time variation of the measured maximal velocity and obtained mean axial velocity, as well as the wall shear stress τ_w and $\tau_{w,\mathrm{S}}$.

Remarks

- The method proposed for the calculation of the axial velocity using the measured maximal velocity requires the assumption of the Wo number associated with heart frequency.
- The discrepancy of maximal and mean axial velocity is high. Because of that, the estimation of blood flow rate in blood vessels by using the maximal velocity is poor.
- The proposed method offers a good estimation of the mean velocity and wall shear stress.

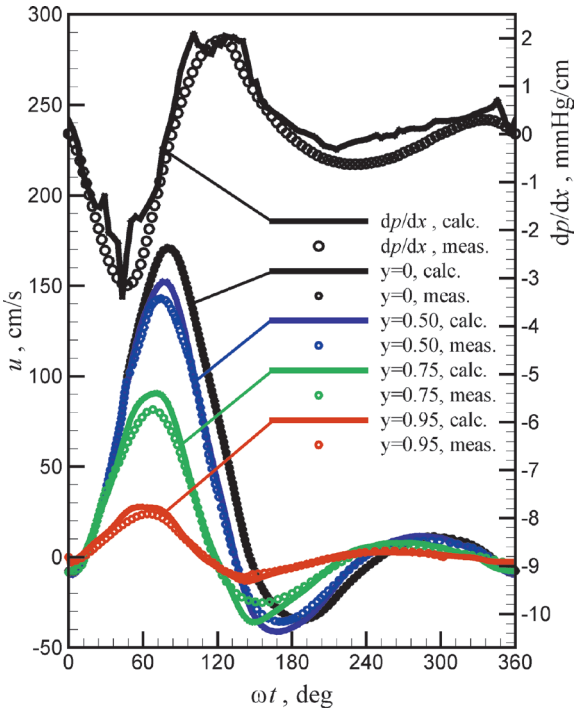

Fig. 1. Measured and calculated pressure gradient and axial velocity at different radii

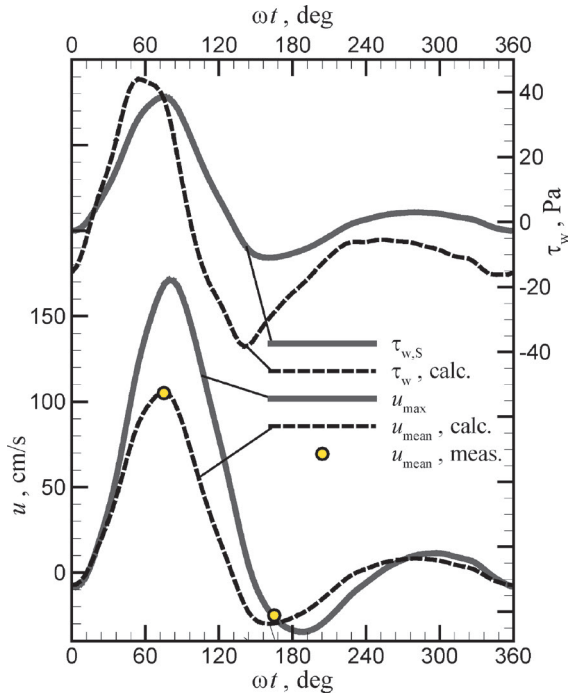

Fig. 2. Comparison between two wall shear stresses and measured maximal velocity with calculated mean axial velocity. Two points denote the measured values of maximal and minimal mean axial velocity

References

[1] Womersley, J.R., "Method for the Calculation of Velocity, Rate of Flow and Viscous Drag in Arteries when the Pressure Gradient is Known, J. Phys. No.127, 1955, 553-563.

[2] Nichols, W.W; O'Rourke, M.F.: McDonald's Blood Flow in Arteries, (5th ed.) Oxford Univ. Press, New York, USA, 2005.

Vedrana Markučič, Severino Krizmanić, and Ante Jurčević

Hemodynamics of Abdominal Aortic Aneurysm

University of Zagreb, Faculty of Mechanical Engineering and Naval Architecture

Introduction

Hemodynamics of abdominal aortic aneurysm (AAA) is presented. AAA is a permanent dilatation of abdominal aorta. The majority of AAAs contain intraluminal thrombi (ILTs) which have an active role in growth and remodeling of AAA [1], [2], [3].

Geometry of ideal fusiform AAA observed here is axisymmetric and cylindrical. In order to examine the impact of geometric variations on hemodynamics, different maximum luminal radii (R) of ideal fusiform AAA models were tested. The time averaged wall shear stress (TAWSS) is the parameter that can be used to predict ILT accumulation [4], [5]. Generally, ILT is accumulated when TAWSS on luminal surface is less than 0.4 Pa [6]. Using computational fluid dynamics, we can model blood flow and study the TAWSS through different AAA, and thus predict ILT accumulation. The aim of this study is to define minimal R (denoted by R_{cr}) where ILT starts to accumulate.

Models and Methods

Geometry models of AAA

The full geometrical model consists of the aorta segment, the aneurysm segment and the bifurcation segment (Fig. 1). The geometry of the aorta and the bifurcation segment are constant while the aneurysm segment evolves due to local elastin loss [7].

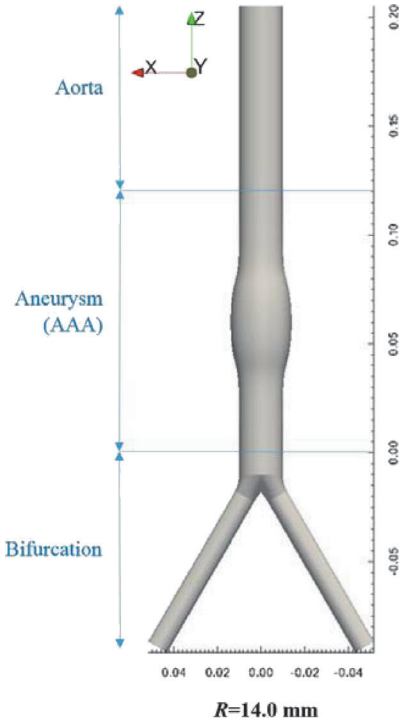

Fig. 1. Full geometrical model

Due to two symmetry planes, we examined 1/4 of the full model. The Salome software platform was used for geometry model generation and the final model is exported in form of a STL file describing its boundaries (inlet, outlet, symmetry and wall). After that the model is meshed in cfMesh program. The finite volume meshes for different R consists from 40000 to 50000 control volumes. Each of the finite volume meshes is hex-dominant. In the inner space of AAA model, the size of control volumes is 1 mm, while near the walls the size is 0.1 mm.

Hemodynamic simulation

Hemodynamic simulation was performed to determine whether an ILT will be deposited, as well as to predict the location and the amount of its accumulation. Thrombus accumulation is predicted based on TAWSS at the luminal surface lower than 0.4 Pa [6].

The time-dependent (pulsatile) volume flow with the parabolic velocity profile, based on data presented in Olufsen et al. [8], is defined on the inlet boundary. Blood is modeled as incompressible (ρ = 1060 kg/m^3) non-Newtonian fluid described by Carreau–Yasuda model [9], [10].

A numerical computation of the laminar transient flow was performed using SIMPLE algorithm for unsteady problems, implemented as "pimpleFoam" program in OpenFOAM software package. The discretization of the mathematical model was linear-upwind (second-order upwind), while the time integration method was Crank-Nicholson.

In each hemodynamic simulation five cardiac cycles were calculated with variable time step. The duration of one cardiac cycle was 1 second. First four cardiac cycles were used to evolve cyclicality of cardiac cycle and to accomplish velocity convergence. Results from the last (fifth) cycle were used to obtain the average wall shear stress (TAWSS). TAWSS distribution was computed on a 0.01 seconds sample (100 time values) within the fifth cardiac cycle and circumferentially averaged.

Results and Discussion

Fig. 2 shows TAWSS along z coordinate (z-axis is centerline of AAA) for different maximum luminal radii (R). The region with the lowest TAWSS corresponds to the region of a larger AAA diameter.

For R of 12 mm and 12.5 mm, the previously mentioned criterion of ILT accumulation is not fulfilled (no area with TAWSS lower than 0.4 Pa). At R of 13 mm the first TAWSS lower than 0.4 Pa appears and this is the maximum luminal radius (R_{cr}) where the first ILT will be accumulated. The larger ILT will be accumulated for R larger than R_{cr} due to a larger area of AAA where TAWSS is lower than 0.4 Pa. R of 14 mm also has

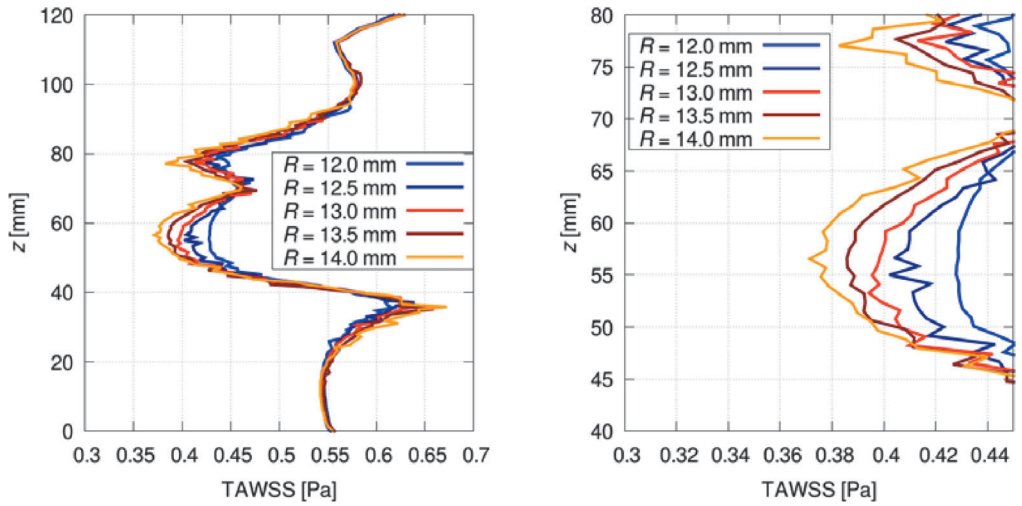

Fig. 2. TAWSS along z-axis (centerline) for different maximum luminal radii

the second area of AAA where TAWSS is lower than 0.4 Pa, thus the second ILT accumulation zone is generated. Fig. 3 illustrates the ILT accumulation zones (blue).

Conclusion

The hemodynamic analysis provides a valuable insight into the blood flow of AAA, providing a prediction of the ILT accumulation based on the time averaged wall shear stress (TAWSS). In the cases observed the critical maximum luminal radius was found to be from 12.5 to 13 mm. An increase in R results in an enlargement of the ILT accumulation zone. If R is greater than 14 mm, the second ILT accumulation zone occurs.

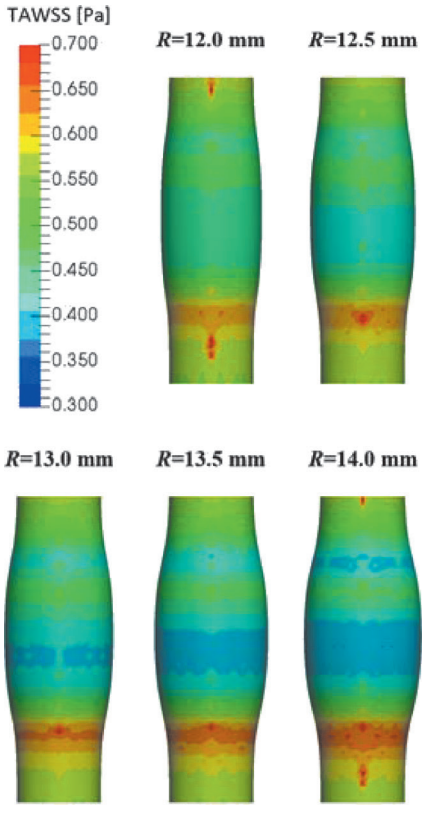

Fig. 3. TAWSS for different R

References

[1] J. S. Wilson, L. Virag, P. Di Achille, I. Karšaj, J. D. Humphrey, Biochemomechanics of intraluminal thrombus in abdominal aortic aneurysms, Journal of Biomechanical Engineering, 135:21011-1-21011–14, 2013.

[2] L. Virag, J. S. Wilson, J. D. Humphrey, I. Karšaj, A computational model of biochemomechanical effects of intraluminal thrombus on the enlargement of abdominal aortic aneurysms, Annals of Biomedical Engineering, 43:2852–2867, 2015.

[3] N. Horvat, B. Zambrano, S. Baek, I. Karšaj. Numerical Modeling of Fluid Solid Growth in Abdominal Aortic Aneurysm. 5th International Conference on Computational and Mathematical Biomedical Engineering – CMBE2017. 2017.

[4] C. Basciano, C. Kleinstreuer, S. Hyun, E. A. Finol, A relation between near-wall particle-hemodynamics and onset of thrombus formation in abdominal aortic aneurysms, Annals of Biomedical Engineering, 39:2010–26, 2011.

[5] P. Di Achille, G. Tellides, C. A. Figueroa, J. D. Humphrey, A hemodynamic predictor of intraluminal thrombus formation in abdominal aortic aneurysms, Proceedings of the Royal Society A, 470:20140163, 2014.

[6] B. A. Zambrano et al., Association of intraluminal thrombus, hemodynamic forces, and abdominal aortic aneurysm expansion using longitudinal CT images, Annals of Biomedical Engineering, 1–13, 2015.

[7] J. S. Wilson, S. Baek, J. D. Humphrey, Parametric study of effects of collagen turnover on the natural history of abdominal aortic aneurysms, Proceedings. Mathematical, Physical, and Engineering Sciences / the Royal Society, 469:20120556, 2013.

[8] M. S. Olufsen, C. S. Peskin, W. Y. Kim, E. M. Pedersen, A. Nadim, J. Larsen. Numerical simulation and experimental validation of blood flow in arteries with structured-tree outflow conditions, Annals of Biomedical Engineering, 28:1281-1299, 2000.

[9] F. J. H. Gijsen, F. N. Van De Vosse, J. D. Janssen, Wall shear stress in backward-facing step flow of a red blood cell suspension, Biorheology, 35:263–279, 1999.

[10] J. Biasetti, F. Hussain, T. C. Gasser, Blood flow and coherent vortices in the normal and aneurysmatic aortas: a fluid dynamical approach to intraluminal thrombus formation, Journal of the Royal Society Interface, 8:1449-1461, 2011.

HATZ News

Activities of the Croatian Academy of Engineering (HATZ) in 2017

Auspices, (Co-)Organization of Conferences and Meetings of Public Interest

Auspices

- 10th Scientific and Professional Colloquium „Textile Technology and Economy 2017"– „Complementarity of Science, Technology and Design", Faculty of Textile Technology in Zagreb, January 24, 2017
- 7th International Scientific and Professional Conference „Water for All" on the occasion of the World Water Day, Faculty of Civil Engineering in Osijek, March 9-10, 2017
- International Colours Day 2017, Technical Museum „Nikola Tesla" in Zagreb, March 21, 2017
- 5th International Congress „Mechanical Engineers' Days", Hotel Olympia in Vodice, March 29-31, 2017
- Faculty of Mechanical Engineering and Naval Architecture in Zagreb, University North, Croatian PLM Association – International Scientific Conference MOTSP 2017 (Management of Technology – Step to Sustainable Production), Dubrovnik, April 5-7, 2017
- Croatian Biotechnology Society – „European Biotechnology Congress 2017", Dubrovnik, May 25-27, 2017
- International Scientific and Professional Colloquium „International Conference on Traffic Development, Logistics & Sustainable Transport" – New Solutions and Innovations in Logistics and Transportation, Opatija, June 1-2, 2017
- Croatian Energy Society – „Hrvoje Požar" Foundation Awards and Scholarships Ceremony, HAZU, Zagreb, July 5, 2017
- Croatian Cartographic Society – 13th Colloquium „Geoheritage, Geoinformation and Cartography", Selce, September 7-9, 2017
- University of Split, Faculty of Electrical Engineering, Mechanical Engineering and Naval Architecture in Split and Croatian Association for Communication and Information Technologies – 25th International Scientific Conference on Software, Telecommunication and Computer Networks SoftCOM 2017, Hotel Radisson Blu, Split, September 21-23, 2017
- Centre for Computer Vision of the University of Zagreb and Faculty of Electrical Engineering, Mechanical Engineering and Naval Architecture – 6th Croatian Computer Vision Workshop, Split, September 26, 2017
- Faculty of Food Technology in Osijek, Croatian Food Agency, 10th International Scientific and Professional Meeting „With Food to Health", Osijek, October 12-13, 2017
- Faculty of Electrical Engineering, Computing and Information Technologies in Osijek – International IEEE Conference on Smart Systems and Technologies 2017 (SST 2017), Osijek, October 11-13, 2017
- Faculty of Food Technology in Osijek – 9th International Congress and 11th Croatian Congress of Flour Production and Processing Technologists „Flour-Bread '17", Opatija, October 25-27, 2017
- Croatian Energy Society – 26th Forum: Energy Day in Croatia, Museum of Contemporary Art, Zagreb, November 17, 2017
- Scientific Centre of Excellence for Data Science and Co-operative Systems – "2nd Int'l Workshop on Data Science (IWDS 2017)", Faculty of Electrical Engineering and Computing in Zagreb, November 30, 2017

(Co-)Organization of Conferences

- 7th Joint Session of the Council and Co-ordination of Four Academies (Croatian Academy of Medical Sciences, Croatian Academy of Legal Sciences, Croatian Academy of Engineering and Academy of Forestry Sciences), Zagreb, January 30, 2017
- Croatian Academy of Engineering – Department of Chemical Engineering and Centre for Environmental Protection and Development of Sustainable Technologies, PLIVA Croatia, Inc. and Model, Ltd. – Scientific and Professional Conference „Application of Mathematical Modelling and Numerical Simulation in the Chemical Process Industry", Zagreb, February 23, 2017
- Croatian Engineering Association, Croatian Academy of Engineering and Faculty of Forestry in Zagreb – Croatian Engineers' Day, Zagreb, March 2, 2017
- Croatian Academy of Engineering – Department of Graphical Engineering and Centre for Graphical Engineering – International Scientific Symposium „Printing&Design 2017", Zagreb, Školska knjiga, March 9, 2017
- Croatian Academy of Medical Sciences, Croatian Academy of Legal Sciences, Croatian Academy of Engineering and Academy of Forestry Sciences – Scientific Symposium „Modern Technologies: Ethics of Usage and Legal Regulation", Zagreb, Croatian Physicians' Assembly, March 17, 2017
- HATZ and ICENT – Round Table Discussion „Today's Challenges in the Energetics", Zagreb, FER, April 24, 2017
- Croatian Academy of Engineering and Public Open University Zagreb – Round Table Discussion "Teachers' Competences in the Higher Education" and Promotion of the Book "Curricular and Didactic-methodical Grounds of the Higher Education Teaching" (authors: Duško Petričević, PhD, Prof. Gojko Nikolić, PhD, Daniel Domović, BSc Comp, and Jelena Obad, BSc Psych), Zagreb, FSB, March 28, 2017.
- HATZ – Round Table Discussion "Status and Future of Technological and Biotechnological Sciences in Croatia in the 21st Century", Zagreb, FER, May 8, 2017
- HATZ – 32th Annual (Elective) Assembly of the Croatian Academy of Engineering, Zagreb, Great Hall of the University of Zagreb May 15, 2017
- Euro-CASE Board Meeting, Paris, France, June 13, 2017
- CAETS 2017 Convocation, Real Academia de Ingeniería (RAI), Madrid, Spain, November 12-19, 2017
- HATZ – Committee for Economic and Regional Co-operation, Croatian Chamber of Economy and Innovation Centre Nikola Tesla – Round Table Discussion „THE EXPERIENCES AND GUIDELINES IN THE IMPLEMENTATION OF MAJOR PROJECTS IN THE FIELD OF ENERGETICS", Zagreb, Croatian Chamber of Economy, November 20, 2017
- 9th/7th Joint Session of Joint Session of the Council and Co-ordination of Four Academies (Croatian Academy of Medical Sciences, Croatian Academy of Legal Sciences, Croatian Academy of Engineering and Academy of Forestry Sciences), Zagreb, AMZH, November 27, 2017
- HATZ and Zagreb Innovators' Association – Educational Workshop „Innovations and Patents", Zagreb, HATZ, November 29, 2017

- HATZ – Department of Communication Systems and FER – Lecture of Prof. Oscar Quevedo-Teruel, PhD (KTH Royal Institute of Technology, Stockholm, Sweden), "Higher symmetries for the design of periodic structures", Zagreb, FER, December 5, 2017
- HATZ – Committee for Ethics and Department of Textile Technology with Faculty of Textile Technology in Zagreb – Lecture of Assoc. Prof. Tomislav Krznar „Ethics and Ecology – A Contribution to Development of the New Knowledge Paradigm", Zagreb, TTF, December 5, 2017
- HATZ – Committee for Economic and Regional Co-operation, Croatian Chamber of Economy and Innovation Centre Nikola Tesla – Round Table Discussion "DEVELOPMENT AND APPLICATION OF ROBOTICS IN CROATIA", Croatian Chamber of Economy, Zagreb, December 6, 2017
- HATZ – Scientific Councila and Faculty of Electrical Engineering and Computing – Lecture of Academician Božidar Liščić "Research, Development and Further Construction of Wind Power Plants in the World", Zagreb, FER, December 7, 2017
- HATZ – Department of Graphical Engineering and Centre for Graphical Engineering with Faculty of Graphical Engineering in Zagreb – Lecture of Prof. Dr. Rajendrakumar Anayath (International Member of HATZ in the Department of Graphical Engineering, Vice Chancellor Deenbandhu Chhotu Ram University of Science and Technology – DCRUST, Haryana State Government University, India), "BRINGING AGILITY IN TECHNICAL EDUCATION TO SUSTAIN AND DEVELOP, Zagreb, GFZ, December 8, 2017
- HATZ – Department of Communication Systems and FER – Lecture of Prof. Antonio Šarolić, PhD (Faculty of Electrical Engineering, Mechanical Engineering and Naval Architecture, Split), "Electromagnetic Impact of Wind Turbines on the Functionality of Vicinal Radars", Zagreb, FER, December 15, 2017
- HATZ – 3rd Session of the Presidency of the Croatian Academy of Engineering and Christmas Reception, Zagreb, Home of the HATZ, December 18, 2017
- HATZ – Department of Communication Systems and FER – Lecture of Prof. Tin Komljenović, PhD (University of California, Santa Barbara, SAD), "Integrated Photonics for LIDAR and Communications", Zagreb, FER, December 19, 2017

Participation at the Meetings of Public Interest

- Christmas and New Year Reception of the Croatian Chamber of Mechanical Engineers, Zagreb, January 20, 2017
- Croatian Academy of Sciences and Arts and Faculty of Architecture in Zagreb – Scientific Colloquium „Models of Revitalization and Advancement of Cultural Heritage", Zagreb, May 2017
- Faculty of Textile Technology – 14th Assembly of the AMCA TTF, Zagreb, June 6, 2017
- Lecture of Tihomir Domazet, PhD, „Development of Croatia on the Economics and Technology Shaping the 21st Century Society", Great Hall of the University of Zagreb, July 19, 2017
- Hanza Media – Jutarnji list Conference „Croatian Defense Industry as an Export Brand", Hotel Esplanade, Zagreb, September 5, 2017
- HAZU – Exhibition „Gutenberg and the Slavic World", HAZU, September 20, 2017
- Lecture of Prof. Bruno Zelić, PhD, „Development of an Integrated Microsystem for Biocatalytic Production of Biodiesel", HAZU, Zagreb, September 21, 2017
- Promotion of the Book „Speleology"with the Exhibition „Researchers of the Croatian Subsoil", HAZU, Zagreb, September 25, 2017
- Lecture „Century of Research of the World of Atoms", HAZU, Zagreb, September 26, 2017
- AMZH Forum „Challenges of Micronutrition in Medicine" (Lecturer: Prim. Sanja Gregurić, MD), Croatian Physicians' Assembly, Zagreb, September 26, 2017
- AMZH Round Table Discussion „Future of Biomedical Sciences in Croatia", Croatian Physicians' Assembly, Zagreb, September 29, 2017
- HAZU and Croatian Association of Petroleum Engineers and Geologists – 9th International Conference and Exhibition on the Petroleum and Gas Economy and Primary Energy, Solaris, Šibenik, October 3-4, 2017
- Faculty of Transport and Traffic Sciences Day, Zagreb, October 9, 2017
- Croatian Innovators' Association and National and University Library in Zagreb – 15th International Innovation Exhibition – ARCA 2017, and the 9th International Fair of Innovation in the Agriculture, Food Industry and Agricultural Mechanization – AGRO ARCA 2017, Zagreb, NSK, October 17, 2017
- Faculty of Forestry Sciences Day, Zagreb, October 20, 2017
- University of Zagreb Day (Dies Academicus), Zagreb, November 3, 2017
- International Innovations and Business Plans Exhibition „Be a Paragon/Inova 2017", Zagreb, November 9-11, 2017
- National and University Library in Zagreb – Exhibition „The Renaissance Faustus Verantius" on the Occasion of the 400th Anniversary of Death of Faust Vrančić, Zagreb, NSK, November 6-25, 2017
- Faculty of Architecture in Zagreb – 10th Days of the Passive House in Croatia, Zagreb, November 10, 2017
- 9th Colloquium of the Croatian Academy of Sciences and Arts and Croatian Science Foundation – "Hierarchically coordinated administration of major consumers with the aim of their integration in the advanced energy network" (Lecturer: Assoc. Prof. Mario Vašak, PhD), Zagreb, HAZU, November 13, 2017
- University of Zagreb, Croatian Academy of Sciences and Arts and School of Medicine in Zagreb – Colloquium „Innovations in Medicine VI", Zagreb, HAZU, November 15, 2017
- Croatian Academy of Sciences and Arts, Croatian Academy of Medical Sciences, Clinical Hospital Centre Rijeka, Faculty of Medicine in Rijeka – 15th Scientific Forum "Role of Oral Health in General Health", Rijeka, MEFRI, November 17, 2017
- Croatian Academy of Medical Sciences, Infective Diseases Clinic „Dr. Fran Mihaljević", School of Public Health Andrija Štampar et al. – Symposium on the Occasion of the European Antibiotics Awareness Day and World Antibiotics Awareness Day, Zagreb, November 17, 2017
- Croatian Waters – H_2O SUMMIT 2018, Zagreb, November 20, 2017
- HAZU and HZZ – 10th Colloquium – Lecture of Academician Slobodan Vukičević „Hepcidin Regulation in the Iron Metabolism by Osseous Morphogenetic Protein 6", Zagreb, HAZU, November 22, 2017
- AMZH – Forum „Teranostic Approach to Post-traumatic Stress Disorder"(Lecturer: Prof. Nela Pivac, PhD), Zagreb, Croatian Physicians' Assembly, Zagreb, November 28, 2017

- SLAP – 7th Conference on the River Sava Basin Regulation from the Border with the Republic of Slovenia to Sisak, Zagreb, November 29-30, 2017
- FER – Public Presentation of the Project „Advanced Methods and Technologies in Data Science and Co-operative Systems (DATACROSS)", Zagreb, FER, November 30, 2017
- HAZU – 150th Anniversary of the Croatian Academy of Sciences and Arts and 140th Anniversary of the Annual of the Croatian Academy of Sciences and Arts, Zagreb, December 4, 2017
- HAZU – Scientific Council for Protection of Nature – Lecture of Prof. Ivica Kisić, PhD, „Soil and Natural Disasters", Zagreb, HAZU, December 5, 2017
- HAZU and HZZ – 11th Colloquium of the Croatian Academy of Sciences and Arts and Croatian Science Foundation – Robert Vianello, PhD, "What is Computational Chemistry and How Does it Help Us Fight the Neurodegenerative Diseases?", Zagreb, HAZU, December 7, 2017
- Faculty of Forestry Sciences in Zagreb – International Scientific Conference ICWST 2017, Zagreb, December 8, 2017
- Croatian Academy of Legal Sciences – Scientific Conference „International Penal Law – Succession and the New Challenges", Zagreb, Faculty of Law, December 12-13, 2017
- Professional Discussion „Co-operation of University and Economy – An Example of Good Practice: the ALTPRO Company", within the Forum „Innovation and Technology Transfer – Boosting the Economic Development of Croatia", University of Zagreb, December 13, 2017
- Croatian-Israeli Business Club – Traditional Holiday Reception, Zagreb, Hotel Le Premier, December 13, 2017
- AMZH – Croatian Academy of Medical Sciences Day (Dies Academicus), Zagreb, Croatian Physicians' Assembly, December 13, 2017
- Technical Museum Nikola Tesla – Meeting on the Organization of the 100th Anniversary of Founding the Technical College in Zagreb by the Exhibition in the Technical Museum Nikola Tesla in 2019, Zagreb, TMNT, December 14, 2017
- Croatian Academy of Sciences and Arts – Holiday Reception, Zagreb, HAZU Palace, December 14, 2017
- Society of University Teachers and other Scientists in Zagreb – Traditional Christmas Meeting, Concert and Reception, Zagreb, December 18, 2017
- Geotechnical Faculty in Varaždin – Ceremonial Session on the Occasion of the Geotechnical Faculty Day, Varaždin, December 20, 2017
- Institute of Lexicography Miroslav Krleža – Christmas Reception, Zagreb, LZMK, December 20, 2017
- Croatian Wood Cluster – Christmas Reception, Zagreb, Hotel Westin, December 20, 2017

HATZ Publications in 2017

1. „Annual 2016 of the Croatian Academy of Engineering" (in Croatian), HATZ, Zagreb, 2017

2. HATZ Bulletin in English „Engineering Power" Vol. 12(1) 2017 (single issue)

3. HATZ Bulletin in English „Engineering Power" Vol. 12(2) 2017 / HATZ Bulletin in Croatian „Tehničke znanosti" Vol. 21 (1) 2017 (double issue)

4. Book of Abstracts of the HATZ Round Table Discussion „Status and Future of Technological and Biotechnological Sciences in Croatia in the 21st Century", HATZ, Zagreb, 2017

5. Book of Abstracts of the Scientific and Professional Conference „Application of Mathematical Modelling and Numerical Simulation in the Chemical Process Industry", organized by the Croatian Academy of Engineering – Department of Chemical Engineering and Centre for Environmental Protection and Development of Sustainable Technologies, PLIVA Croatia, Inc. and Model, Ltd., HATZ, Zagreb, 2017

HATZ News Editor
Melanija Strika, Business Secretary of the Croatian Academy of Engineering

Engineering Power – *Bulletin of the Croatian Academy of Engineering* Vol. 12(3) 2017 – ISSN 1331-7210
Publisher: Croatian Academy of Engineering (HATZ), 28 Kačić Street, P.O. Box 59, HR-10001 Zagreb, Republic of Croatia
Editor-in-Chief: Prof. Vladimir Andročec, PhD, President of the Academy
retired Full Professor with tenure, University of Zagreb, Faculty of Civil Engineering
Editor: Prof. Zdravko Terze, PhD, Vice-President of the Academy
University of Zagreb, Faculty of Mechanical Engineering and Naval Architecture
Guest-Editor: Prof. Zdravko Virag, PhD, Member of the Academy in the Department of Mechanical Engineering and Naval Architecture
University of Zagreb, Faculty of Mechanical Engineering and Naval Architecture
News Editor: Melanija Strika, MSSc, Business Secretary of the Academy
Editorial Board: Prof. Vladimir Andročec, PhD, Prof. Zdravko Terze, PhD, Prof. Zdravko Virag, PhD, Melanija Strika, MSSc
Editorial Board Address: Croatian Academy of Engineering (HATZ),
„Engineering Power" – Bulletin of the Croatian Academy of Engineering, Editorial Board,
28 Kačić Street, P.O. Box 59, HR-10001 Zagreb, Republic of Croatia
E-mail: hatz@hatz.hr
Graphical and Technical Editor: Vladimir Pavlić, Dipl. Eng. (GRAPA, Ltd., Zagreb) *Press:* Tiskara Zelina, Ltd., Zelina
Proof-reader: Miroslav Horvatić, MA *Circulation:* 300